Volume 1 | Number 1 | Jan 2013 | Pages 1–100

Journal of
Materials Chemistry B

Materials for biology and medicine
www.rsc.org/materialsB

ROYAL SOCIETY
OF CHEMISTRY

ROYAL SOCIETY
OF CHEMISTRY

www.rsc.org/materialsB

Short Text: Multilevel structures of electrospun membranes can be controlled and the designed structures can strongly affect cell behavior and drug delivery.

Electrospun membranes: control of the structure and structure related applications in tissue regeneration and drug delivery

Haiyan Li[1], Yachen Xu[1], He Xu[1], Jiang Chang[1,2*]

[1]Med-X Research Institute, School of Biomedical Engineering, Shanghai Jiao Tong University,

1954 Huashan Road, Shanghai, 200030, China

[2] Shanghai Institute of Ceramics, Chinese Academy of Sciences, 1295 Dingxi Road, Shanghai

200050, China

*Corresponding author:

Jiang Chang

Tel.: +86-21-52412804;

Fax: +86-21-52413903;

E-mail address: jchang@mail.sic.ac.cn

Address: Shanghai Institute of Ceramics, Chinese Academy of Sciences, 1295Dingxi Road,

Shanghai 200050, China.

Abstract

This article presents an overview focusing on the structure control of electrospun membranes in multilevel scale, from morphology of single nanofibers, packing and alignment of nanofibers to patterns and shape of fibrous scaffolds. Typical structures of electrospun membranes and specific electrospinning strategies used to produce these structures have been reviewed. In addition, potential applications of these controlled structures in tissue engineering and drug delivery have been highlighted. Finally, this review concludes with perspective on challenges and future directions for design and fabrication of electrospun scaffolds with controlled structures, and for investigation of the relationship between structures of electrospun membranes and cell behaviors as well as drug delivery behaviors.

Keywords: Electrospinning; structure control; tissue engineering; drug delivery

1. Introduction

Electrospinning technology has been widely applied in preparation of fibrous membranes as cell scaffolds and drug delivery carriers due to its simplicity, capacity to form fibers on both the micro and nano scale, cost-effectiveness, flexibility, potential to scale up, and ability to spin broad range of polymers [1]. Usually, electrospinning technology requires four major components: a syringe pump, a high-voltage power generator, a spinneret with a metallic needle and a grounded collator [2]. As there is strong electrical potential applied to polymer liquid (solution or melt), the surface of liquid droplet at the tip of the needle is covered by electrical charges. When the electric field strength overcomes the surface tension of the droplet at a critical voltage, a charged jet is ejected from the tip of the droplet. The jet is elongated and whipped continuously by electrostatic repulsion until it arrives on the grounded collector [2]. During this process, the solvent gets evaporated, and the jet gets solidified. Finally, the resultant fibers were collected and formed a nonwoven fibrous membrane.

Electrospun nanofibrous membranes have certain remarkable characteristics, such as the high surface area-to-volume ratio, high interconnected porosity with tunable pore size, possibilities for efficient surface functionalization, adjustable surface morphology, and structural similarity to the extracellular matrix (ECM) [3, 4]. With the above mentioned characteristics, electrospun nanofibers and membranes have been widely used in tissue engineering, drug delivery and medical diagnosis

[5]. In tissue engineering, a scaffold to provide a three dimensional (3D) support for cell attachment, proliferation and tissue formation is required. The natural ECM, consisting of various interwoven protein fibers with diameters ranging from tens to hundreds of nanometers, support cells and guide cell behavior [6]. Electrospun scaffolds have great potential to mimic the important features of natural ECM in terms of structural, chemical and mechanical properties [7, 8].

In addition to being used as cell scaffolds in tissue engineering, another important application of electrospun membranes is drug delivery system due to the above mentioned remarkable characteristics as well as its ability to provide the opportunity for direct encapsulation of drugs into the electrospun fibers. Electrospun membranes with nanofibers containing various models of drugs have been fabricated and their drug delivery behaviors have been widely studied [4]. Either hydrophilic or hydrophobic drugs and biomacromolecules, such as proteins and DNA, can be incorporated into the electrospun fibers [9-13]. The advantages of electrospun membranes as drug delivery system are higher drug-encapsulation efficiency, less efficient drug dosage, controlled release behavior via proper selection of a drug-polymer-solvent system or electrospinning parameters as compared to other forms of drug carriers, such as liposome, nano/microspheres and hydrogels produced by conventional methods [4, 13].

Electrospun membranes were firstly prepared with randomly arranged nanofibers and structures, while structural characteristic of the electrospun membranes has been found critical for many applications [5, 14, 15]. As most native ECM found in tissues or organs possesses anisotropic architecture, to improve the function of regenerated tissue, structural biomimetic substitutes have recently been developed to precisely imitate native ECM for repairing damaged tissue [15]. Construction of electrospun membranes with biomimetic structure can be achieved by controlling the electrospinning parameters [15-20]. A variety of electrospun membranes with fascinating structures resembling natural objects, such as lotus leaf, rice leaf, honeycomb, polar bear fur, spider webs, ECM, etc., have been fabricated by selecting proper composition and structures of electrospun fibers [7, 19, 20]. More and more literatures have reported that electrospun membranes with anisotropic structure and controlled microstructure of nanofibers possess more desirable properties and show greater advantages as compared to those with random structures in their biomedical applications, especially in tailoring cell behaviors in tissue engineering and controlling drug release [10, 21-26].

This article gives a brief overview of recent work on the design, fabrication and applications of electrospun membranes with controlled multilevel hierarchical structures for tissue engineering and drug delivery applications with highlightening the effects of the structures on cell behavior and drug release. In addition, perspectives as well as challenges and future directions of the study in the development of electrospinning technology for more accurate and complicate structural control and potential applications of electrospun membranes with controlled structures are proposed.

2. Control of the structure of electrospun membranes

2.1 Microstructure control of single electrospun nanofiber

Diameter, morphology and secondary structures of electrospun nanofibers are the basic structures of nanofibers that form an electrospun membrane. The structure of nanofiber is dependent on a number of parameters, which mainly include the intrinsic properties of solution for electrospinning, the electrospinning parameters and the surroundings where the electrospinning happens [17]. The intrinsic properties of solution are affected by the viscosity/concentration of the solution, polymer type, polymer chain conformation, polymer molecular, electrical conductivity of the polymer as well as polarity and surface tension of the solvent while the electrospinning parameters include the intensity of the electrical field, the distance between the needle tip and collector, and the feeding rate for the polymer solution. Besides, the local humidity, temperature and wind velocity also strongly affect the morphology and diameter of electrospun nanofibers [27].

2.1.1 Electrospun nanofibers with core/sheath structure

Usually, electrospun nanofibers exhibit a solid interior and smooth surface. However，by controlling the electrospinning parameters, nanofibers with specific secondary structures can be achieved. With different electrospinning setups and conditions, electrospun nanofibers with core/sheath structures have been fabricated [7, 9, 10, 28-30]. One method to prepare nanofibers with core/sheath structure is electrospinning of blended polymer solution [29], which is simple and straightforward, but requires a good miscibility between core and sheath liquids. Briefly, a blend polymer solution containing two types of polymers is prepared first. When the polymer solution is electrospun and the phase separation happens during the electrospinning process, a nanofiber with core/sheath structure can possibly be obtained. Wei et al. used this method to prepare core/sheath

nanofibers with poly(butadiene) (PB) in the center and poly(carbonate) (PC) locating outside by electrospinning of PB/PC blended solution and carefully selecting proper processing conditions and compositions [29].

Mixing two different polymers at the liquid jet during electrospinning process is another method to obtain nanofibers with core/sheath structure. The principle of this method is that the low diffusion coefficients of polymer chains and quick electrospinning process limit good miscibility of two polymer solutions during the electrospinning process [1]. Therefore, a compound liquid jet can be obtained when the two polymer solutions meet at the jet and subsequently nanofibers with core/sheath structures will be formed. Based on this principal, co-electrospinning method has been used to prepare nanofibers with core/sheath structure from two different polymers by a coaxial two-capillary spinneret [28, 31-34]. Sun et al. used this method to obtain Poly(ethylene oxide) (PEO, shell) / poly(dodecylthiophene) (PDT, core) and PEO (shell) /polysulfone (PSU, core) core-sheath nanofibers [28]. However, the yield and uniformity of the core/sheath structure are affected by all processing parameters, including viscosities, immiscibility, and composition of both core and sheath liquids. For example, if the two polymers are well miscible, it is hard to obtain core/sheath compound liquid jets with good yields due to mixing of two polymers. In comparison to electrospinning of blended polymer solution, the co-electrospinning method does not need good miscibility of two polymer solutions, which is easier for selecting materials and suitable for different kind of materials. However, the co-electrospinning method requires relative complicate electrospinning setups.

2.1.2 Electrospun nanofibers with hollow structure

It has been demonstrated in many literatures that nanofibers with hollow interiors, for example, nanotubes, are very important for various applications, e.g. nanofluidics, hydrogen storage, and biomedical applications [34]. Various methods have been developed to fabricate such structures and electrospinning is one of the methods that can directly fabricate hollow nanofibers without complicate procedures [2, 30, 34-40]. With electrospinning method, nanofibers with hollow structures are usually fabricated from nanofibers with core/sheath structures by removing either the core or sheath material. Xia and Li firstly prepared a poly (vinyl pyrrolidone) (PVP)/ heavy mineral oil nanofibers with PVP in the sheath and oil in the core. PVP nanotubes can be obtained by extracting the mineral oil in the core with a solvent such as octane or polycrystalline ceramic

nanotubes can be obtained by removing PVP from the wall through calcination. This method also shows advantages in preparing metallic oxides and ceramic nanotubes using heat treatment due to the high thermostability of the materials [34]. Through sacrificing of organic polymer template at high temperature during calcination, formation of hollow ceramic or metallic oxide nanofibers can be obtained. For example, Xia et al. proposed an one-step method for fabrication of SnO_2 hollow nanofibers by directly annealing PVP/Sn precursor and subsequently removing PVP by heat treatment [37].

However, preparation of hollow nanofibers through removing one component in nanofibers with core/sheath structure usually requires relative complicate procedures and only works well for relatively short nanofibers as it is easy to get overlapping or entanglement between long, flexible templates and finally results in interconnections between the hollow fibers [34]. To overcome the problems, Wu et al. developed a novel method to prepare nanocrystalline hydroxyapatite assembled hollow fibers (NHAHF) in an electrospun membrane by combining the electrospinning technique and the hydrothermal treatment [40]. In this method, electrospun bioactive glass fibers (BGF) were used as self-sacrificial templates. During the hydrothermal method, the electrospun BGF served as a structure-directing scaffold and a precursor for growth of the shell. In addition, the solution used for hydrothermal process could dissolve the BGF during the shell-forming process. Therefore, hollow NHAHF nanofibers could be obtained with its growth from BGF and the dissolution of BGF itself. To prepare hollow fibers with this method, careful selection of material and control of electrospin parameters are required. Various inorganic or organic electrospun nanofibers can be used as precursors and templates. In addition, the hydrothermal process and conditions are critical, which directly determine the structure and composition of hollow inorganic nanofibers. Inorganic hollow nanofibers with different compositions can be obtained through this method if the hydrothermal process is carefully controlled.

Coaxial electrospinning technology has been applied to prepare hollow nanofibers with multilayer wall. Wei et al. fabricated hollow ultrafine fibers with a multilayer wall using coaxial electrospinning technology in one step [41]. By carefully choosing the polyethersulfone (PES) dissolved in dimethyl sulfoxide (DMSO) as shell solution and both of dilute hydrophilic polyethylene glycol (PEG) and polyvinyl alcohol (PVA) dissolved in DMSO as core solutions, hollow fibers with two different layers (porous structure layer and dense smooth layer) could be

obtained due to the phase separation during the electrospinning process [41]. Hollow nanofibers with multilayer wall show advantages in controlling drug delivery due to the co-existence of porous layer and dense smooth layer.

2.1.3 Electrospun nanofibers with porous structure

Porous structure can provide nanofibers a much larger surface area as compared to nanofibers with solid structure, which is of interest for catalysis, filtration, absorption, fuel cells, solar cells, batteries, tissue engineering as well as drug delivery [30, 36, 37, 42-44]. Porous structures of nanofibers can be developed by several methods. One method is the selective removing of a component from solid nanofibers made of composite or blend materials [45]. Another method is the induction of phase separation of different polymers during electrospinning by choosing proper electrospinning parameters [46]. Fabricating porous nanofibers using a coaxial, double-capillary electrospinning system is a recently developed method [34].

For example, Bogntizk et al. prepared nanofibers with porous structures by electrospinning from ternary solutions using polylactide (PLA) and PVP as polymer model components and dichloromethane as solvent and selectively removing one of the components after phase separation by carefully controlled processing parameters [45]. Rabolt and co-workers have demonstrated that the pore size and morphology of porous nanofibers could be controlled by adjusting the humidity and solvent vapor pressure in atmosphere after electrospinning a variety of crystalline and amorphous polymers, including PC, PEO, poly(methyl methacrylate) (PMMA), and polystyrene (PS) [47]. Recently, Xia and Li applied a coaxial, double-capillary system and polymer phase separation to prepare porous ceramic nanofibers [34], in which PS was firstly dissolved in a mixture of dimethylformamide (DMF) and tetrahydrofuran (THF) solvent as the core liquid and PVP was dissolved into Ti(OiPr)$_4$ as the sheath liquid (Fig. 1 (D)). PS and PVP are immiscible but the DMF/THF and Ti(OiPr)$_4$ are miscible. During electrospinning process, these two polymer phases were separated and a continuous matrix of TiO$_2$/PVP formed with nanoscale domains of PS embedded. After the PS were removed by calcination, porous TiO$_2$ nanofibers were obtained, which is shown in Fig.1(E).

The common requirement of all these three methods is the need to carefully select the polymer systems and removal of one component after solid nanofibers are formed to generate a porous structure. The first method needs to choose two polymers with good miscibility in order to

electrospin a blended polymer solution. The second method needs to choose two polymers that can be induced to phase separate during the electrospinning process. The third method, however, needs to choose two polymers that are immiscible but the two solvents are miscible in order to get a partially mixed solution during the electrospinning process, so that the two polymer phases are separated after the solvent evaporation. After the solid nanofibers are obtained by these three methods, one component of the fibers is removed by dissolving or heat treatment and porous structure in nanofibers can be generated.
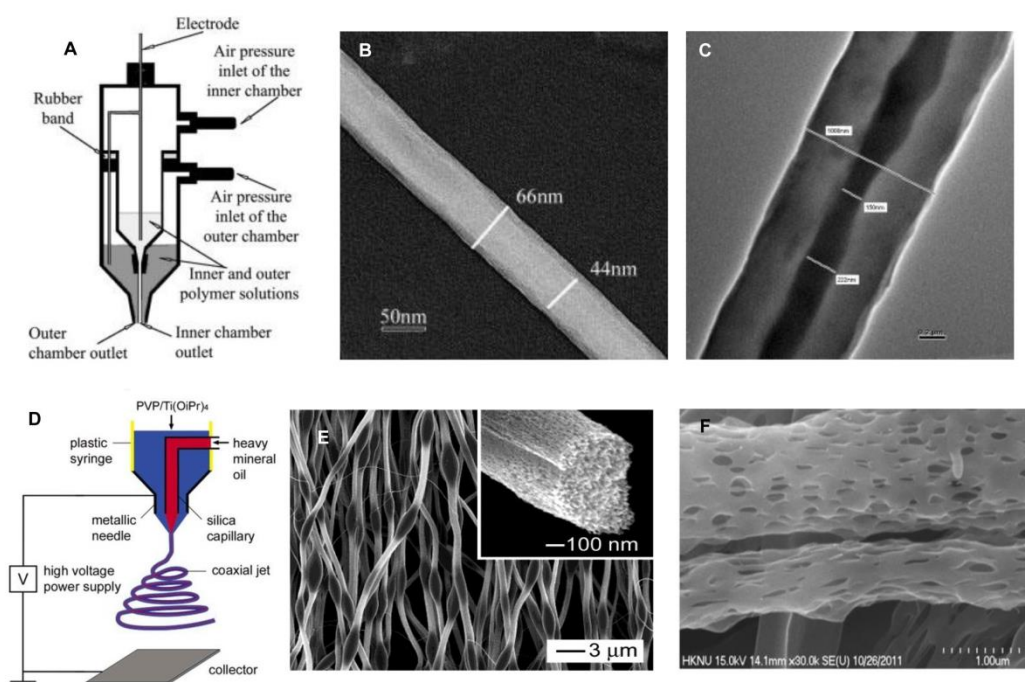
Fig. 1 (A) Experimental setup used for co-electrospinning of compound core-shell nanofibers. (B) TEM of a compound nanofibers. Core and shell solutions are PSU and PEO, respectively. (C) TEM of unstained samples of co-electrospun PEO (shell) and PDT (core). Images in (A), (B) and (C) were reprinted with permission from [28]. Copyright (2003) WILEY-VCH Verlag GmbH & Co. (D) Schematic illustration of the setup for electrospinning nanofibers having a core/sheath structure. The spinneret was fabricated from two coaxial capillaries, through which heavy mineral oil and an ethanol solution containing PVP and Ti(OiPr)4 were simultaneously ejected to form a continuous, coaxial jet. (E) SEM images of TiO2 fibers fabricated by electrospinning, with a DMF/THF solution of PS (0.12 g/mL) as the core and an ethanol solution of Ti(OiPr)4/PVP (0.3 and 0.03 g/mL, respectively) as the sheath. Images in (D) and (E) were reprinted with permission from [34]. Copyright (2004) American Chemical Society. (F) Field emission-scanning electron microscopy image of porous salicylic acid + poly(ethylene

glycol)/PLA core/sheath composite nanofibers fabricated at core feed rates of 0.2 mL/h. This image were adapted with permission from [43]. Copyright (2012) Elsevier.

2.1.4 Control of nanofibers diameter

It has been widely accepted that fiber diameter can influence cell adhesion, proliferation, migration, and differentiation [48] since cells actually interact with the protein absorbed on the materials when mammalian cells interact with biomaterials. During the interaction, signaling is transferred into cells and the assembly of focal adhesion contacts are leaded [49]. Then, cells exert contractile forces on materials, and signaling pathways inside cells are activated, which can finally regulate cell proliferation and phenotype [17, 27, 48]. The diameter of nanofibers, however, affects the protein absorption and the assembly of focal adhesion contacts, which subsequently influences the signaling activation and transfer. Therefore, controlling diameter of nanofibers is critical for controlling cell behaviors. Many parameters can affect the diameter of electrospun fibers, including polymer properties, solution properties, electrospinning process conditions, and ambient parameters [49]. Through controlling these parameters, the diameter of electrospun fibers can be controlled over a range from 150 nm to 5 μm [17, 27]. This range of diameters is much smaller than that of fibers formed by convention extrusion processes and wet spinning processes as well as mammalian cells, which is in the range of feature sizes that can facilitate contact guidance [49].

For controlling diameter of electrospun nanofibers, various methods have been developed through adjusting polymer properties, solution properties, electrospinning conditions and ambient parameters. Du et al. added iron acetylacetonate into polyacrylonitrile solution for controlling fiber diameter by selectively adjusting solution properties. They found that, with increased salt concentration, the fiber diameter increased to a peak value due to changes in solution viscosity, conductivity, and surface tension. In addition, the operational conditions also influence fiber diameter as fiber diameter increases with increase in voltage, feed rate, and spinneret-collector distance [50]. Toompson et al. investigated the effects of different materials and operating parameters on electrospun fiber diameters and their results demonstrated that the jet radius as well as the fiber diameters were significantly affected by five parameters, i.e. volumetric charge density, distance from nozzle to collector, initial jet/orifice radius, relaxation time, and viscosity. The other parameters (initial polymer concentration, ionic strength, solution density, electric potential, perturbation frequency, and solvent vapor pressure) have moderate effects on the jet radius while

relative humidity, surface tension, and vapor diffusivity have minor effects on the jet radius [51-53].

2.1.5 Control of fibers combined with beads and particles

Sometimes, electrospun membranes are composed of not only fibers with smooth surfaces, but also fibers with beads or particles [1, 54-57]. Electrospun fibers with beads are unexpected at most time, although it has been observed very often[54, 55]. At least three forces, including surface tension, electrostatic repulsion force, and viscoelastic force, dominate the bead formation during the electrospinning technology[1]. Generally, formation of beads can be avoided if the balance between these three forces can be achieved, i.e. the influence of surface tension can be suppressed by the effects of the electrostatic repulsion force and viscoelastic force. The three forces are intrinsically affected by the polymer properties and solution properties, which mainly includes polymer molecular, solution concentration as well as salt content in polymer solution [54, 55]. For example, Xia and Li reported that bead density sharply reduced when the concentration of PVP was increased. When a small amount of tetramethylammonium chloride was added into PVP solution, bead-free PVP nanofibers could be obtained [1]. Besides, applied electrospinning voltage has also been confirmed to be correlated to the formation of bead in the electrospun fibers [54, 55].

Electrospun fibers with particles embedded within fibers are also called "islands in the sea" [56, 57], which is another interesting phenomenon during preparation of electropsun fibers. Fibers with "islands in the sea" structure are usually formed with phase separation during electrospinning process. Huang and co-workers prepared poly(lactic acid) (PLA) homopolymer and poly(p-dioxanone)-b-poly(ethylene glycol) multi-block copolymer (PPDO-b-PEG) nanofibers through single spinneret electrospinning. Through controlling the crystallization and subsequently the phase separation in the obtained nanofibers, different phase separation morphologies in nanofibers could be obtained, including fibers with smooth surface, fibers with "sea-island" structure and fibers with core-shell structure [57].

2.2 Control of fiber packing and orientation of electrospun membranes

2.2.1 Control of fiber packing

Electrospun membranes have been tried to be applied as cell scaffolds in tissue engineering. However, the conventional electrospinning method usually form a non-woven scaffolds, which are composed of tightly packed 3D sheet-like structures. Many literatures indicated that these sheet-like, tightly packed 3D structures with small fiber diameters actually only allow cells to

grow and migrate on the superficial surface. Therefore, the scaffolds actually act like a 2D membrane and the cells only interact with the surface but not penetrate into the inner parts of electrospun scaffolds. In addition, the densely packed fibers of the electrospun scaffolds not only restrict the cell infiltration but also limit nutrient exchange and metabolic waste removal throughout the scaffolds, which can finally result in necrosis and unsuccessful or incomplete regeneration of tissues [16, 58-60].

To overcome these problems, several strategies have been tried to increase the porosity and pore size of the electrospun scaffolds. Mixing two components in the electrospun membranes and removing one of them after electrospinning can result in low packing density of nanofibers. For example, combination of salt particulate leaching or fiber sacrificing with electrospinning technology has been used to reduce packing density of nanofibers, which is a simple method and has achieved moderate success [58, 60-63]. Kim et al. fabricated a 3D macroporous and nanofibrous hyaluronic acid (HA) scaffold with this salt leaching method [58], in which the salt particulates as a porogen were simultaneously deposited on the fibers during electrospinning process. The subsequent chemical cross-linking and salt leaching resulted in a HA-based scaffold retaining a macroporous and nanofibrous geometry. The fiber sacrificing method is similar to the salt leaching approach, in which two different kinds of fibers with different chemical or physical properties are co-electrospun together and one type of the fiber is sacrificed by leaching out in post-processing based on its specific properties to form voids throughout the electrospun scaffolds. In general, the scaffolds prepared by this method have large pore size and high porosity, which is beneficial for facilitating cell infiltration. Baker et al. used this method to prepare a highly porous polycaprolactone (PCL) scaffold by removing PEO from a composite PCL/PEO electrospun membrane [62], which can be seen from Fig. 2. Phipps et al. used this method to obtain PCL/collagen I (Col I)/nanoparticulate hydroxyapatite (HAp) composite scaffolds for bone tissue engineering with PEO as sacrificial fibers [63].

Besides, reducing the packing density of electrospun nanofibers with designed collectors or post-treatments during or after the electrospinning process is also a useful method to increase the porosity of electrospun scaffolds for cell infiltration. For example, Blakeney et al. developed a 3D cotton ball-like electrospun membrane that consists of nanofibers in a low density and uncompressed manner using a grounded spherical dish and an array of needle-like probes as

collectors [64]. In another study, a porous mandrel was tried to produce a scaffold with low density with an air-impedance process [65]. Besides, Lee et al. used an ultrasonication method to mechanically separate the fibers, resulting in large pore size and low fiber density, and the porosity of electrospun nanofibers was highly enhanced [42].

Increasing diameter of nanofibers is another commonly used method to increase the pore size and porosity of electrospun scaffolds [66, 67]. Mixing nanofibers with microfibers has also been tried to produce porous electrospun scaffolds. For example, electrospinning has been used to coat single microfiber with nanofibers to take full advantages of electrospun nanofibers and microfibers [67]. Wu et al. obtained a scaffold with yarns by depositing and twisting electrospun nanofibers into yarns in a water vortex before collecting on a rotating mandrel [59].
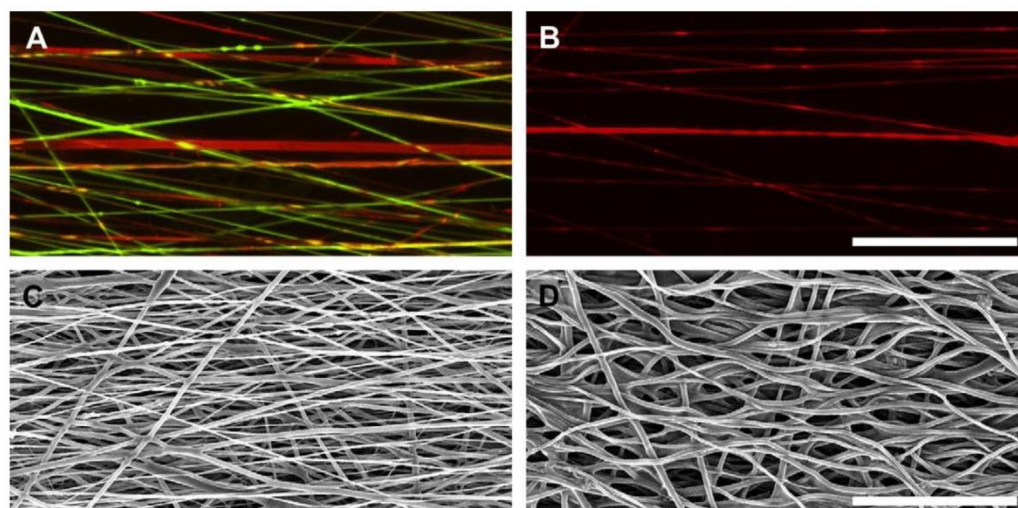
Fig. 2 Composite fibrous scaffolds can be formed with individual fibers of distinct polymer composition. Removal of one sacrificial fiber population increases scaffold porosity. (A) Fluorescently-labeled PCL (red) and PEO (green) fibers showed pronounced alignment and interspersion. (B) Submersion of scaffolds in an aqueous solution removed the PEO component but left the PCL fibers intact. SEM images of as-spun (C) and post-submersion (D) composite scaffolds revealed increases in pore size with the removal of sacrificial PEO fibers. Scale bars: 50 mm. Images reprinted with permission from [62]. Copyright (2008) Elsevier.

2.2.2 Control of fiber orientation

Electrospun nanofibers are typically collected as non-woven membranes with random fiber orientation because of the bending instability associated with a spinning jet. However, in some applications, especially in tissue engineering, orientation or alignment of nanofibers is required as most native ECM in tissue or organs have anisotropic architecture. Recently, various approaches

have been tried to realize different types of orientations, such as axial, yarn and radial orientation [7, 18, 21, 24, 68-70]. Fiber orientation can be induced by electrospinning onto a rotating drum [71, 72], disc [25], between two grounded rods [73], or by two oppositely placed metallic needles [70].

The straightforward method is to use a cylinder, for example, a drum, rotating with high speed as a collector, to obtain orientated electrospun fibers [71, 74]. Some assistant methods, such as the help of air flow, could improve the orientation of nanofibers along the wind direction. However, it is hard to obtain perfect orientation of nanofibers simply with a drum collector [1]. To improve the orientation of nanofibers, wheel-like disk collector has been applied as the strength of electrostatic field increased significantly near the edge of the disk. Then, the collected fibers could be well-aligned in parallel to each other along the edge of the disk [75]. For instance, Xu et al. aligned poly(l-lactide-co-e-caprolactone) [P(LLA-CL)] nanofibers with a rotating disk collector with a sharp edge to obtain fibers with diameter of 500 nm for mimicking the circumferential orientation of cells and fibrils found in the medial layer of a native artery [25]. Since then, a number of studies have been reported on fabrication of well-aligned nanofibers using similar setups with slight modifications on the collectors [46].

According to above results, it can be concluded that the geometrical configuration of a conductive collector has a strong effect on the orientation of electrospun fibers. Therefore, Xia et al. explored a pair of splited collector consisting two conductive strips separated by a void gap of variable widths to uniaxially align nanofibers over long length scales during the electrospinning process, which is shown in Fig. 3 [73, 76]. They studied the effect of the area and geometric shape of the insulating gap on the deposition of fibers. Both their experimental and theoretical work clearly demonstrated that the introduction of an insulating region into a conductive collector influenced the electrostatic forces acting on a charged fiber, which finally determined the alignment of the nanofibers. Their results indicate that, with the aid of electrostatic interactions, electrospun nanofibers can be assembled into controllable structures with different configurations by simply changing the design of the collector. For example, uniaxially aligned fibers can be directly collected on a conducting surface by controlling the configuration of the electrode [77]. Based on this principal, an electrospun nanofibrous scaffold consisting radially aligned PCL nanofibers has been developed by utilizing a collector composed of a central point electrode and a peripheral ring electrode in order to imitate the dura mater and to develop artificial dura substitutes to promote

cell migration from the surrounding tissue to the center of a dura defect [78].

The above two methods are based on the design of the geometrical configuration of collectors, which indicates that the collectors play a key role in preparation of aligned electrospun fibers. Besides, other parameters of electrospinning process, such as viscosity and conductivity of polymer solution, also have significant influences on the degree of the fiber alignment. Song et al. demonstrated that addition of inorganic salt into polymer solution affected the alignment of the electrospun fibers [79]. They added three kinds of inorganic salts (Ca(NO3)2· 4H2O, MgCl2· 6H2O, CaCl2) into poly(vinylbutyral) (PVB) solution to study the effects of different kinds of salts on fiber alignment. The results demonstrated that the fiber alignment was significantly influenced by both viscosity and conductivity of the solutions, while the viscosity and conductivity of the solutions were affected by the addition of inorganic salts. The increase of the conductivity of the solution resulted in the increase of fiber orientation degree [79].
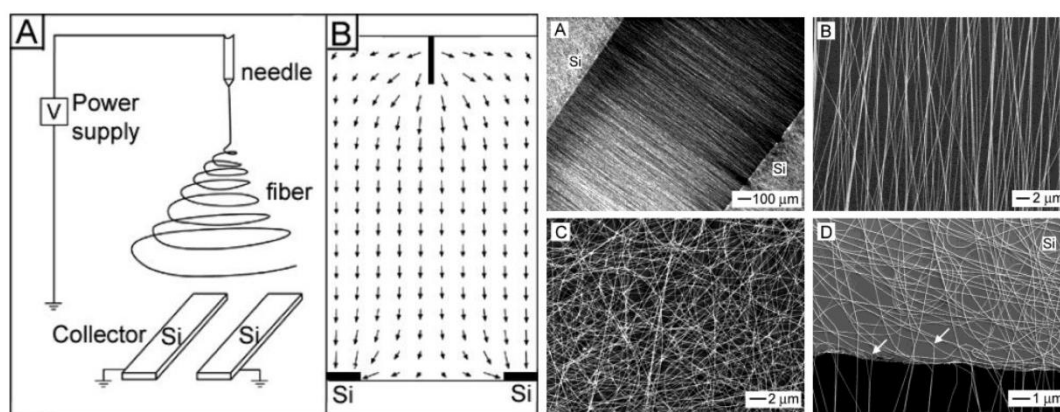
Fig. 3 Left panel: (A) Schematic illustration of the setup used for electrospinning uniaxially aligned nanofibers. Two pieces of conductive silicon stripes separated by a gap was used as the collector. (B) shows the analysis of electric field strength vectors in the region between the needle and the collector. The arrows indicated the direction of the electrostatic field lines. Right panel: SEM images show the orientation of PVP nanofibers in different regions of collectors. (A) Dark-field optical micrograph of PVP nanofibers collected on top of the gap between two silicon stripes in the collector. (B, C) SEM images taken from the same sample, showing nanofibers deposited (A) across the gap and (C) on top of the silicon stripe. (D) SEM image of another sample taken from a region close to the edge of the gap. All images were reprinted with permission from [73]. Copyright (2003) American Chemical Society.

2.3 Fabrication of electrospun membranes with patterned structure

Recently, electrospun membranes with complex ordered architectures and patterns have attract more and more attention as controlling the pattern of nanofibers (as well as their stacking into hierarchical structures) is important for many applications [7, 14]. Zhang et al. developed a new method using electroconductive templates to fabricate electrospun mats with controllable architectures and patterns [80]. Electroconductive wires and metal collector with square-shaped protrusions were applied to design patterned collectors. They demonstrate that the pattern of the wires and protrusions in an electroconductive collector greatly affected the pattern structures of the electrospun mats.

Different from the method used by Xia et al. where insulating quartz wafers were used as the collecting substrates and gold electrodes of different designs and feature sizes were patterned in the center of these quartz wafers to obtain patterned electrodes, zhang et al. simply used electroconductive templates to obtain patterned collectors and subsequently achieved patterned electrospun nanofibers. In terms of the mechanism, the configuration of electroconductive collectors changes the electric field and forces. Subsequently, the deposition of nanofibers is affected. Zhang et al. also suggested that protrusions play an important role in controlling the arrangement of the fibers on the electroconductive collectors. Their results showed that, when a electroconductive collector with some electroconductive protrusions was used, fibers were only deposited randomly on the protrusions and in parallel between the most adjacent protrusions, which suggested that the surface topography of electroconductive collector could affect the orientation of the electrospun fibers, and a patterned architecture could also be generated using a continuous conductive collector with patterned protrusions.

Besides, by changing the surface architectures and distribution of collectors, electrospun nanofibers could be easily assembled into well-ordered nanofiber meshes comprising both types of topographies, i.e. random and parallel alignment of nanofibers co-existed in the same mesh [15, 60, 81, 82]. Based on this method, electrospun membranes with various pattern structures have been developed [15, 60, 82]. Fig. 4 shows the electrospun membranes with various patterns prepared with this method and the effects of the electrospinning parameters on those patterns. Xu et al. used this method to prepare composite D,L-poly(lactic acid) (PDLLA)/PCL scaffolds with uniform crisscross pattern using patterned collector with square-shaped protrusions and they showed that the order degree of the pattern of PDLLA/PCL electrospun mats could be finely tuned by

controlling blending ratios between PDLLA and PCL, which subsequently changed the conductivity of the fibers [83].

Besides design of collectors, post-treatments have also been applied to generate patterns in electrospun membranes. For example, to mimic the native ECM of anterior cruciate ligament (ACL), electrospun membranes with crimp-like pattern were developed by soaking as obtained electrospun membranes into phosphate buffered saline (PBS) at a temperature higher than the Tg of the polymer fibers, which resulted in the release of the stress and contract of the fibers to form a wavy, crimp-like microarchitecture [22, 84, 85]. Therefore, the crimp-like pattern was obtained after the as-spun aligned but un-crimped nanofibers were soaked overnight in PBS with a temperature of 10 $^{\circ}$C higher than the Tg of the polymer. During the electrospinning process, fibers were stretched and residual stress was remained in the fibers. The wave pattern possesses an amplitude of 5 μm and a wavelength of 46 μm, which are similar as that of native ACL collagen matrix[22].
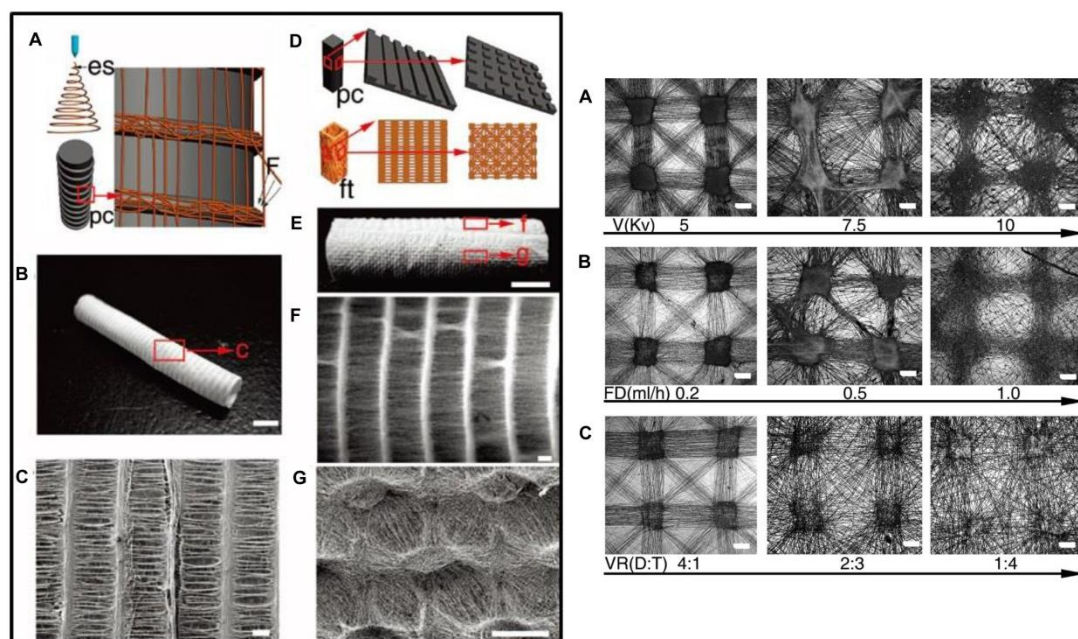
Fig. 4 Left panel: (A) Schematic illustration of collecting process using a cylindrical collector with equally spaced circular protrusions (es, electrospinning process; pc, patterned collector). (B) A fibrous tube with patterned architectures (scale bar = 5 mm). (C) Magnified image of B (scale bar = 200 μm). (D) Schematic illustration of collectors with two different patterns and relevant fibrous tube (pc, patterned collector; ft, fibrous tube). (E) A fibrous tube with two different patterns (scale bar = 5 mm). (F-G) Magnified images of two different patterns of E (scale bar = 200 μm). Right panel: (A) Influence of voltage on patterned architectures (v, voltage). (B) Influence of feeding rate on patterned architectures (FD, feeding rate). (C) Influence of volume ratio of solvents (DMF/THF)

on patterned architectures (VR, volume ratio; D, DMF; T, THF). (scale bar =100 μm). All images were reproduced from [82]. Copyright (2008) American Chemical Society.

2.4. Three dimensional shape control of electrospun membranes

To imitate the hierarchical architecture and mechanical characteristics of native tissue ECM, electrospun membranes have been fabricated into special shapes/structures. For example, for vascular or neural tissue engineering, scaffolds with tubular conduit structure are important. Traditional tubular scaffolds possess limited surface area, which cannot host a large number of cells needed for complete and faster regeneration of tissues while tubular scaffolds with electrospun nanofibers provide a solution to this problem through increasing the surface area, mimicking the ECM and finally increasing cellular attachment and proliferation on the scaffolds [86, 87]. Numerous vascular prosthetics composed of nanofibers with various polymers have been fabricated using electrospinning technology. Normally, a circular mandrel was made to rotate and translate during fabrication to ensure even deposition of fibers and the obtained scaffolds were cross-linked in order to increase the stability and strength of the scaffolds [87, 88]. Stitzel et al. fabricated tubular scaffolds from a PLGA, collagen and elastin mixture solution using a rotating mandrel with a diameter of 4.75 mm and rotation rate of 500 rpm. They achieved vascular prosthetics with adequate mechanical strength and elasticity and appropriate bioactivity, which have similar mechanical properties to those of a native vessel [88].

Recently, tubular electrospun scaffolds with aligned or patterned nanofibers attract more and more interest. Through controlling the rotating speed of the mandrel, tubular electrospun scaffolds with simply aligned nanofibers could be obtained. For example, when the rotating speed of a mandrel reached to 3000 rpm, electrospun tubular scaffolds with aligned nanofibers could be obtained [87]. However, to achieve the high rotating speed of mandrel, sophisticated setups are required. Collecting nanofibers with a rotating mandrel and two parallel auxiliary electrodes is another promising way to obtain tubular scaffolds with aligned fibers without using high rotating speed of mandrel [86, 89]. For example, Wu et al. used two separated metallic plates with a distance of several centimeters apart to prepare electrospun small PCL nanofibrous tubular scaffolds with circumferential, axial, and combinations of circumferential and axial directions aligned nanofibers through controlling the electrospinning parameters and collector setups [89].

However, the above methods can only produce tubular scaffolds with aligned nanofiber but

are difficult to generate patterned nanofibers in the tubular scaffolds. To solve this problem, Zhang et al. develops a method to fabricated 3D nanofibrous tubes with different architectures using designed collector templates, which is a simple and straightforward method that does not need complicate electrospinning setups [82]. Through designing different protrusions on a rotating collector, single tubes with multiple micropatterns and multiple interconnected tubes with same or different sizes, shapes, structures and patterns could be easily fabricated, which has been partially shown in Fig. 4 [82].

Besides tubular nanofibrous scaffolds, spiral structured nanofibrous scaffolds have been fabricated to mimic the structure of bone for bone tissue engineering or to improve neural regeneration [90, 91]. In those studies, the spiral 3D structure of nanofibrous scaffolds were simply produced by manually oriented or rolled an electrospun membrane in a concentric manner with an open central cavity. For example, to mimic the hierarchical architecture and mechanical characteristics of native ECM of bone, Deng and co-workers fabricated a scaffold possessing both advantages of electrospun nanofibers and 3D hierarchical bone architecture and bone mechanics through producing a spiral scaffolds from electrospun nanofibers [90]. The process for fabricating the unique scaffolds are illustrated in Fig. 5 (upper panel) and the obtained spiral shape scaffolds are shown in Fig. 5 (down panel, a-c). Briefly, biocompatible dipeptide polyphosphazene-polyester blended nanofibrous matrices with nanofibers of diameter ranging from 50 nm to 500 nm were electrospun in order to mimic dimensions of collagen fibrils present in the natural bone ECM. Then, to replicate bone marrow cavity as well as the lamellar structure of bone, blend nanofiber matrices were oriented in a concentric manner with an open central cavity. The stress–strain curve of this obtained scaffold is similar to that of native bone and the compressive modulus of the scaffold is in the midrange of values for human trabecular bone.
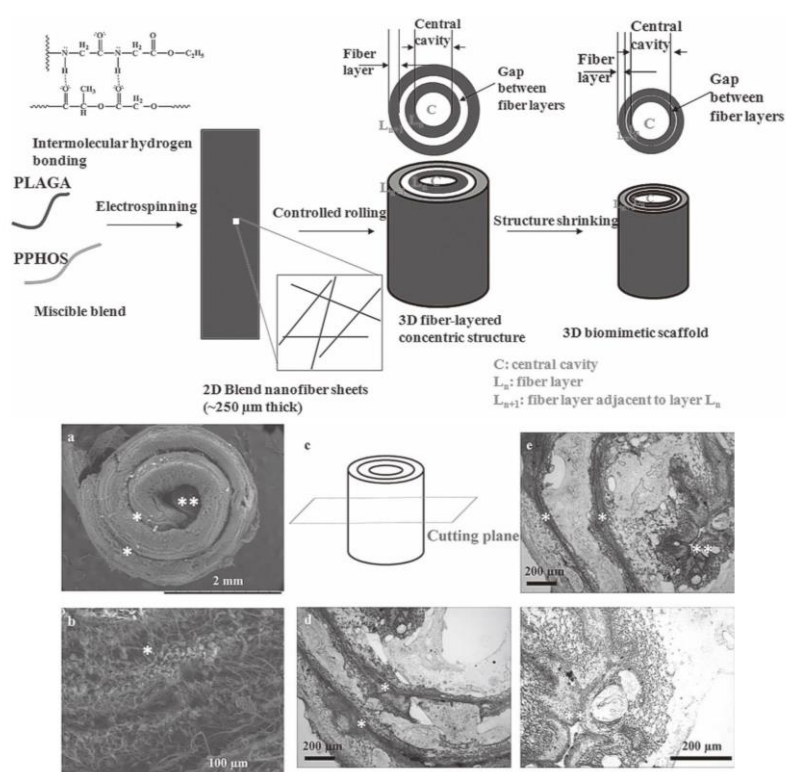
Fig. 5 Upper panel: schematics of 3D biomimetic scaffold design and fabrication. Down panel: ECM deposition throughout 3D scaffold architecture during cell culture. (a–b) SEM images showing the morphologies of cell-seeded 3D biomimetic scaffolds after 28 days of culture: (a) Cell layers covering the scaffold; and (b) ECM deposited by the cells bridging the gaps of concentric pattern by 28 days. Cells could migrate through 250 μm thick concentric fiber laminates from both the surfaces leading to a homogeneous ECM deposition and cellular activity throughout the biomimetic scaffold. (c–f) Immunohistochemical staining for osteopontin (OPN), a prominent component of the mineralized ECM, illustrating a homogenous ECM distribution throughout the scaffold at day 28. (c) Schematics of the select plane for immunohistochemical staining. (d, e) A robust stain for OPN bridging the gap between the concentric layers for the lower portion as well as upper and center portion of the 3D biomimetic scaffold. (f) Higher magnification image of the central cavity showing the robust stain for OPN. (∗) indicates inter-lamellar space whereas (∗ ∗) indicates central cavity. After 28 days, the scaffolds showed a similar ECM organization to that of native bone. Reprinted with permission from [90]. Copyright (2011) WILEY-VCH Verlag GmbH & Co.

3. Electrospun membranes: biomedical applications

3.1 Application of electrospun membranes in tissue engineering

Electrospun membranes, possessing nanofibers and porous structure, have been widely applied in various tissue engineering as their structures are similar to native ECM in many tissue types. It has been widely reported that electrospun membranes are suitable for cell adhesion, proliferation and differentiation in terms of the chemical and physical properties of membranes. However, since ECMs of different tissues have different unique nanofibrous characteristics and more and more evidences demonstrate that micro-to-nanoscale topography of substrates affects cell behavior, which subsequently determines the tissue regeneration, the importance of substrate topography should not be neglected. Recently, with increasing understanding of the interactions between cells and their microenvironment in tissue, more attention shifts to focus on the structural effects of electrospun membranes on cell behavior and tissue regeneration. Therefore, this part will review recent work focusing on the applications of electrospun membranes with specific structures in tissue engineering, including neural, vascular, bone as well as ligament and tendon tissue engineering.

3.1.1 Electrospun membranes with controlled structures for neural tissue engineering

Multilevel structures of electrospun membranes have been reported to be able to affect neural tissue engineering, from diameter of nanofibers, alignment and patterns of nanofibers, to 3D shape of electrospun membranes. It has been widely reported that neural cells are sensitive to nanofiber diameter [26, 48, 49, 92-94]. For example, Christopherson et al. cultured rat hippocampus-derived adult neural stem cells (rNSCs) on laminin-coated electrospun PES fiber meshes with average fiber diameters of 283 ± 45 nm, 749 ± 153 nm and 1452 ± 312 nm with a very narrower diameter distribution. They found that the fiber diameter of PES mesh significantly influenced rNSC differentiation and proliferation as well as migration. A smaller fiber diameter resulted in higher degree of cell proliferation and spreading and lower degree of cell aggregation [48].

A number of studies have demonstrated that orientation of electrospun nanofibers has profound effects on cell morphology and behaviors, including cell attachment, proliferation, migration, extension and differentiation in various types of tissue engineering [21, 24, 25, 95-99]. Although electrospun membranes with random nanofibers have been widely applied in neural tissue engineering due to its nanofibrous structures [95], more and more evidences suggest that nanofiber alignment in electrospun membranes can induce neural cell migration and extension, which can assist in directing the growth of regenerating axons in neural tissue engineering [21, 96-98].

Aligned electrospun PCL fibers have been reported to be able to provide contact guidance to human Schwann cells, inducing the cell cytoskeleton and nuclei to align and elongate along the fiber axes after 7 days culture and promoting Schwann cell maturation [97], as shown in Fig. 6 (left panel).

However, the above studies focused on the effects of uniaxially aligned nanofibers on neural cells behaviors. It also has been reported that patterns of electrospun nanofibers can determine the patterns of neurite outgrowth from primary dorsal root ganglia (DRG) [100]. Xie et al. reported that, when DRG were cultured on a nonwoven mat of randomly oriented nanofibers, the neurites extended radially outward from the DRG main body without specific directionality. In contrast, when DRG were cultured on parallel array of aligned nanofibers, the neurites preferentially extended along the long axis of fibers. If the cells were seeded at the border between regions of aligned and random nanofibers, the same DRG simultaneously expressed aligned and random neurite fields in response to the underlying nanofibers. More interestingly, when DRG were cultured on a double-layered scaffold with different alignment of fibers in each layer, the neurites were found to be dependent on the fiber density in both layers. As an explanation of the mechanism, authors proposed that the traction force might play an important role in the topographic cue effects of patterned nanofibers [100].

Furthermore, special 3D shape of electrospun membranes, such as spiral or tubular electrospun scaffolds, can also improve neural tissue regeneration as they are able to improve cell infiltration and differentiation[91, 101, 102]. Valmikinathan et al. has reported that poly(lactide-co-glycotide) (PLGA) microsphere-based spiral scaffolds with nanofibrous surface have increased surface areas and possesses sufficient mechanical properties and porosities to support the nerve regeneration process. The authors suggest that the advantage of spiral scaffolds is that the spiral structure has an open architecture that goes evenly throughout the scaffolds, which leaves enough volume for media influx and deep cell penetration into the scaffolds. Therefore, nanofibrous spiral scaffolds promoted attachment and proliferation of Schwann cells as compared to contemporary tubular scaffolds or nanofiber-based tubular scaffolds [91].

Although many efforts have been devoted to study the effects of structure of electrospun nanofibers or membranes on nerve repair in order to find an optimal scaffold for improving nerve tissue regeneration, the scaffolds with controlled structures are far to be applied in clinic. For

example, in 3D shape design, Zhu and co-workers have fabricated bi-layered nerve guide conduits (NGCs), which was composed of random nanofibers as the outer layer and aligned nanofibers as the inner layer [102]. However, there is a central cavity in the NGCs, which is not able to provide contact guidance for neuronal outgrowth and may cause a mismatch between proximal and distal ends [103].
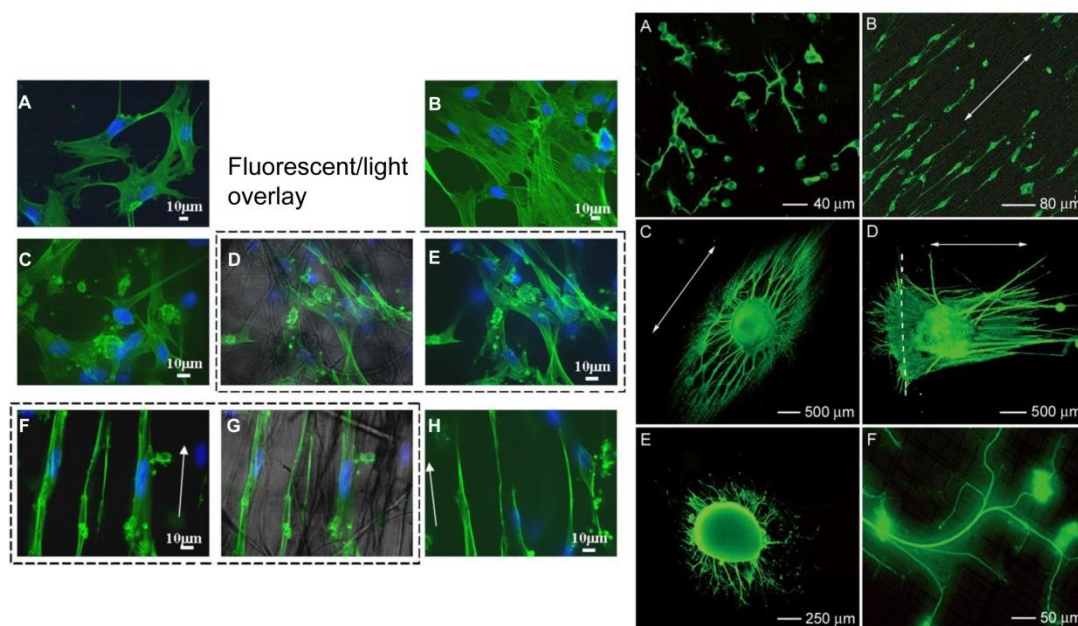
Fig. 6 Left panel: Confocal fluorescent images of human Schwann cells cultured on PCL scaffolds for 3 days (a, c and f) and 7 days (b, e and h). (a) and (b) PCL film; (c), (d) and (e) randomly oriented PCL fibers; and (f), (g) and (h) aligned PCL electrospun fibers, arrows depict directions of fiber alignment. (d) and (g) Fluorescent-light images overlay. Green: actin cytoskeleton, blue: DAPI. These images were reprinted with permission from [97]. Copyright (2008) Elsevier. Right panel: Fluorescence micrographs showing immunostained neurofilament 200 kD in neural stem cells after 2 days of culture: (A) on random nanofibers and (B) on aligned nanofibers. (C) Typical neurite field projected from dorsal root ganglia on aligned poly(3-caprolactone) nanofibers with laminin coating. (D) Typical neurite field projected from dorsal root ganglia at a border between random and aligned poly(3-caprolactone) nanofibers with laminin coating. (E, F) Typical neurite field projected from dorsal root ganglia on a mat of perpendicular poly(3-caprolactone) fibers. All images were reproduced from [95].

3.1.2 Electrospun membranes with controlled structures for vascular tissue engineering

Morphology and alignment of nanofibers as well as 3D shape of electrospun scaffolds have been shown to be able to strongly affect vascular tissue engineering [104-106]. Electrospun membranes with core/sheath structured nanofibers have been reported to be suitable for vascular

tissue engineering. Chen et al. took the advantages of core/sheath nanofibers and applied nanofibrous scaffolds with collagen as sheath and thermoplastic polyurethane nanofibers as core (TPU/collagen) in vascular tissue engineering [105]. They demonstrated that the collagen surface could regulate cell–scaffold interactions when pig iliac endothelial cells (PIECs) were cultured on the scaffolds. Compared with pure collagen and TPU, compound TPU/collagen core/sheath nanofibers could provide better growth condition for cell proliferation because of the good biocompatibility of collagen. In addition, the proper mechanical properties of TPU provide the scaffolds with better mechanical strength as compare to the pure collagen scaffolds.

Besides neural tissue engineering, alignment of blood vessel cells has also been reported to be able to improve vascular tissue engineering [23, 25, 86]. One of the reason is that the smooth muscle cells (SMCs) and collagen fibrils in the medial layer of the natural arteries have a marked circumferential orientation in order to provide the mechanical strength to withstand the higher pressure existing in the circulation [25]. Both SMCs and human venous myofibroblasts used in vascular tissue engineering have been reported to be sensitive to nanofiber alignment in electrospun membranes [23, 25, 86]. Xu and co-workers indicated that parallelly aligned P(LLA-CL) nanofibers strongly affected the behaviors of human coronary SMCs, including cell attachment, migration, contractile phenotype, adhesion and proliferation rate, distribution and organization of smooth muscle cytoskeleton proteins inside SMCs [25]. Wang et al. reported that aligned poly(L-lactide) (PLLA) nanofibers in the inner surface could induce orientation of SMCs, facilitate the differentiation of SMCs to healthy contractile phenotype, which indicates that the inner aligned surface in tube has potential ability to improve vessel tissue engineering [86].

3D shape of electrospun membranes plays an important role in vascular tissue engineering due to the specific tubular shape mimicking natural blood vessels. Previous literatures have demonstrated that tubular electrospun scaffolds could support blood vessel tissue engineering due to proper mechanical property [23, 88]. Stitzel et al. fabricated PLGA/collagen/elastin tubular scaffolds and achieved vascular prosthetics with adequate mechanical strength and elasticity and appropriate bioactivity. Compliance tests demonstrated that the electrospun fiber conduit possesses a similar behavior to that of a native vessel [88]. Recently, tubular structured scaffolds with aligned nanofibers have attracted more and more interest to achieve not only proper mechanical properties but also improved biologic properties for blood vessel regeneration [23, 86, 87].

Wang et al. prepared an electrospun PLLA/polydimethylsiloxane (PDMS) tube with assistance of rotating collector and parallel auxiliary electrode to circumferentially align PLLA fibers in the inner surface of the tube for inducing SMCs orientation and differentiation while to locate PDMS in the outer surface of tube for better compressive property [86]. Del Gaudio et al. reported that PCL/ poly(3-hydroxybutyrate-co-3-hydroxyvalerate) (PHBV) composite tubular scaffolds with random or aligned nanofibers supported survival and growth of rat cerebral endothelial cells. In addition, the fiber alignment of the electrospun tubular scaffolds improved the speed and distribution of cell colonization of the luminal [87].

Tissue engineered vascular grafts must possess two primary characteristics, which are proper mechanical properties to withstand physiological conditions and a confluent endothelialized lumen to resist thrombosis [6]. Although current studies focus on the effects of structure on mechanical properties of the electrospun membrane and have obtained some promising results, more *in vivo* studies are needed to prove the clinic application feasibility of these scaffolds as *in vivo* environment is much more complicate than *in vitro* for a vascular graft. In addition, the effects of membrane structure controlling on endothelialized lumen formation have not been widely investigated. Finally, more complicate structures, such as patterns on graft or aligned fibers mixing with random fibers, should be tested for different cells in different layers of vascular grafts since blood vessel has a typical 3-layered structure.

3.1.3 Electrospun membranes with controlled structures for bone tissue engineering

Diameter of nanofibers has been reported to be able to influence bone forming cell behavior and choosing proper diameter of nanofibers can improve bone tissue regeneration [107]. Badami et al. investigated the effects of diameter of four different kinds of polymer fibers with mean fiber diameters ranging from 0.14 μm to 2.1 μm on the density and differentiation of MC3T3-E1 osteoprogenitor cells. They found that the cell density increased with fiber diameter and cells on 2.1 μm diameter fibers were observed to extend lamella podia along individual fibers and exhibited a higher aspect ratio, consistent with a contact guidance phenomenon [107]. Therefore, when the diameter of fibers ranges from 0.14 to 2.1 μm, MC3T3-E1 osteoprogenitor cells prefer to grow on fibers with larger diameter, which is different from that of neural stem cells. When the diameter of fibers ranges from 283 ± 45 nm, 749 ± 153 nm to 1452 ± 312 nm, neural stem cells prefer to proliferate, migrate and differentiate on nanofibers with smaller diameter (283 ± 45 nm)

than on nanofibers with larger diameter (749 ±153 nm and 1452± 312 nm) [48]. This finding suggests that different cells may prefer different diameters of nanofibers. However, due to the limitation of electrospinning technology, nanofibers with a diameter below 100 nm, in particular, in the range of 10–50 nm, which are close to those in native ECM, are difficult to be fabricated.

Infiltration and uniform distribution of cells in a biodegradable scaffold is a crucial step for the success of overall healing of bone defect in tissue engineering approach, especially for the reconstruction of large bone segments [63], which needs blood vessels to deliver nutrient and oxygen as well as remove metabolic waste for those cells within the scaffolds. However, small pore sizes in 2D electrospun membranes constrain the ingrowth of blood vessels into the scaffolds from surroundings, which finally limits the amount of tissue-ingrowth. Several literatures have demonstrated that 3D electrospun scaffolds with enhanced porosity can significantly improve cell penetration and distribution in various types of tissue engineering, including bone tissue engineering [18, 59-63]. Phipps et al. demonstrated that highly porous PCL/Col I/HAp scaffolds obtaining by sacrificing of PEO in the scaffolds possessed mean pore size of 1826.11 mm^2, which was significantly greater than the scaffolds created without PEO fibers (424 mm^2). The porous scaffolds increased the infiltration of mesenchymal stem cells (MSCs) into the scaffolds during cell seeding, as well as greater infiltration of endogenous cells into highly porous scaffold than into the scaffolds created without PEO fibers from calvarial organ cultures [63].

It is well known that bone possesses a hierarchically organized natural structure. The axis of bone is aligned in the same direction as the longitudinal axis of the collagen nanofibers in the basic structure of bone [18]. As bone has significant anisotropic mechanical properties with highly oriented ECM and bone cells, making a nanofibrous scaffolds with oriented and patterned nanofibers as well as special 3D shape of electrospun scaffolds can not only mimic the natural ECM structure but also stimulate osteoblast cell proliferation and differentiation [15, 24, 108, 109]. Spiral shape of electrospun scaffolds have been proved to be able to improve bone tissue regeneration with the same reason that stimulates neural tissue engineering with spiral structured electrospun scaffolds [109]. In addition, more and more studies focus on the effects of aligned and patterned nanofibers on bone forming cells with the aim to improve bone regeneration. Martins et al. cultured hBMSCs over 7 days on random and patterned PCL nanofiber meshes to verify the influence of the nanofiber mesh topography on cell morphology and distribution, proliferation and

differentiation [15]. They found that the patterned nanofibrous could control cellular morphology, with cell polarity following the established fiber direction as in the area of parallel/uniaxial alignment, and hBMSCs attached and spread along the aligned nanofibers of the patterned fiber meshes, as shown in Fig. 7. The same findings were reported in another study, where hBMSCs maintained their phenotypic shape when seeded on randomly oriented scaffolds while nanofiber orientation in aligned nanofiber meshes could guide actin organization of cells. In addition, the proliferation and differentiation of hBMSCs were influenced by the pattern structure of the scaffolds [108].

From above results, it can be seen that more and more researchers start to realize the importance of controlling the structure of electrospun nanofiber and membranes on improving bone regeneration. However, few studies focused on the effects of structure controlling of nanofiber or membranes on mechanical properties, which should not be ignored since bone scaffolds need to meet certain mechanical properties. Besides, most of the studies focused on electrospun polymeric scaffolds. As the bone tissue consists of both organic and inorganic components, electrospun composite nanofibers and membranes with unique structures should be considered in future studies, which may be a great challenge. In addition, only bone forming cells, such as bone marrow mesenchymal stem cells and osteoprogenitor cells, have been used as cell models to evaluate the effects of nanofiber structure on cell behaviors. However, bone tissue regeneration normally involves several types of cells, such as inflammation cells, bone cells and endothelial cells. Co-culture cell model or more cell types should be considered for evaluating the cell behavior responses to structure changes of nanofibers or membranes.
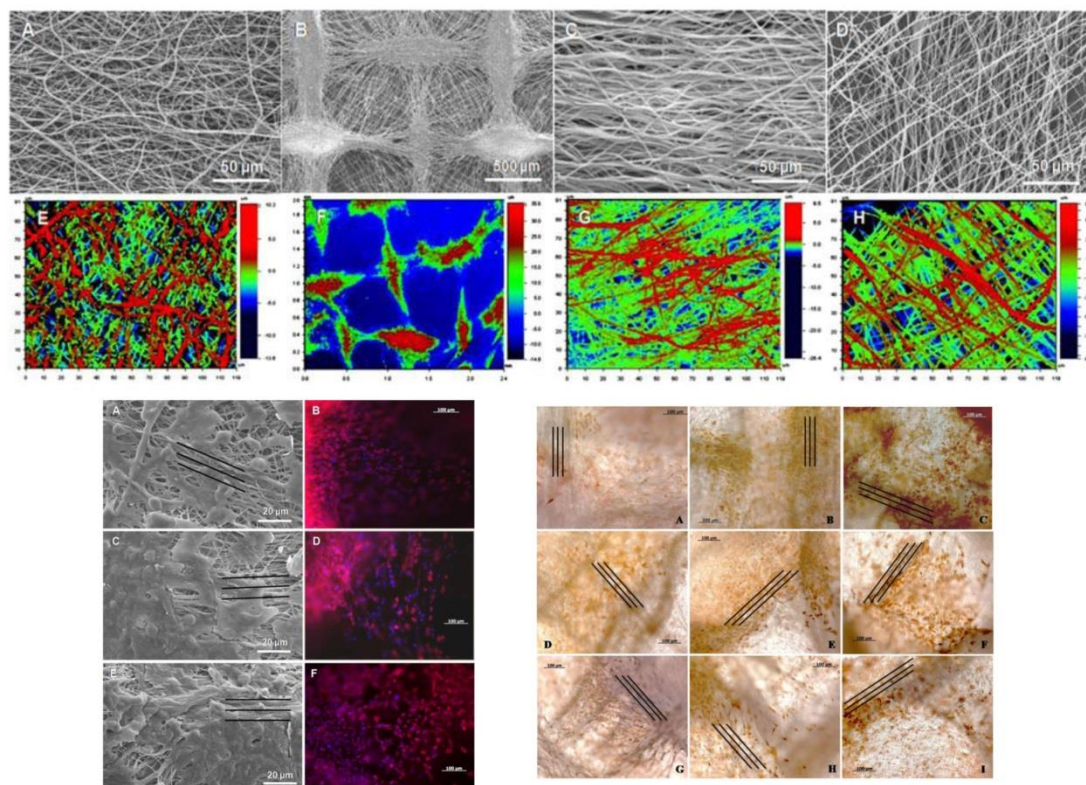
Fig. 7 Upper panel: SEM micrographs (A-D) and optical profilometric images (E-H) of the typical random (A and E) and patterned (B and F) nanofiber meshes. P-NFM comprise areas of parallel/uniaxial (C and G) and orthogonal (D and H) alignment of the fibers. Down left panel: SEM micrographs (A, C and E) and fluorescence images (B, D and F) of hBMSCs induced to differentiate into the osteogenic lineage after 7 (A and B), 14 (C and D) and 21 (E and F) days of culture. Black lines represent the orientation of parallel/uniaxial aligned fibers. Down right panel: Optical images of immunodetected osteogenic markers, namely osteopontin (A–C), bone sialoprotein (D–F) and osteocalcin (G–I), expressed by hBMSCs induced to differentiate into the osteogenic lineage and cultured on patterned nanofiber meshes over 7 (A, D and G), 14 (B, E and H) and 21 (C, F and I) days. Black lines represent the orientation of parallel/uniaxial aligned fibers. All images were adapted with permission from [15]. Copyright (2011) WILEY-VCH Verlag GmbH & Co.

3.1.4 Electrospun membranes with controlled structures for ligament and tendon tissue engineering

Besides the above mentioned bone and vascular tissue engineering, alignment and patterns of nanofibers in electrospun membranes are very critical for ligament and tendon tissue engineering. Crimp-like pattern with a wavelength and amplitude similar to that of native ACL collagen has been demonstrated to be able to improve ligament tissue engineering [22, 84, 85, 110]. Surrao et al.

demonstrated that the scaffolds with crimp-like patterns exhibited improved modulus and underwent a slight decrease in modulus compared to the scaffolds with random deposited polymeric fibers over a 6 month period. In addition, bovine fibroblasts not only grow normally on the scaffolds with crimp-like patterns but also synthesized and deposited ECM in bundle formation that resembled the fascicles found in native ACL [22, 84, 85]. Furthermore, Lee et al. demonstrated that significantly more collagen was synthesized on aligned electrospun nanofiber sheets in the investigation of the effect of nanofiber alignment on the cellular responses of human ligament fibroblasts (HLFs). He further suggested that the HLFs were more sensitive to strain in the longitudinal direction [110].

In tendon tissue engineering, special requirements about the scaffolds structure are needed to be met as tendons attached to bones across a specialized transitional tissue with varying structures and compositions. To imitate the gradients in composition and structure that exist at the natural tendon-to bone insertion, Li et al. fabricated a nanofibrous scaffold with an ''aligned-to-random'' transition in the same scaffold by utilization of a specially designed collector [111]. The scaffolds could not only imitate the structural organization of collagen fibers at the tendon-to-bone insertion site but also guide the tendon fibroblasts to exhibit organized and oriented morphologies on the aligned and random portions, respectively.

Although more and more interests has been focused on generating crimped structures similar to that of native tendon/ligament, the mechanical strength of the obtained scaffold is still much lower than that of native tissue [103], which may cause premature failure of the healing tendon/ligament since tendons and ligaments demand proper mechanical physiological conditions. Future work should focus on improving the mechanical properties of aligned and crimped nanofiber scaffolds.

3.1.5 Electrospun membranes with controlled structures for cartilage tissue engineering

Electrospun membranes with random structure have been reported to be able to support both chondrocytes proliferation and differentiation in many literatures [67, 112-114]. More recently, it has been demonstrated that structures of electrospun nanofibers and membranes, including nanofiber size and alignment [115-118], porosity and pore size of membrane [67, 116, 119] as well as shape of membrane [112, 113, 120], can strongly affect cartilage regeneration. Thorvaldsson and co-workers electrospun PCL nanofibers onto PLA microfibers to combine nanofibers with microfibers in

order to produce highly porous scaffolds for improving cartilage regeneration. They demonstrated that scaffolds with higher porosity significantly enhanced cellular infiltration and the nanofibers supported cell growth in the scaffolds, which is helpful for improving cartilage tissue regeneration [67].

In addition, as cartilage ECM consists of aligned fiber components for withstanding and counterbalancing distinct mechanical load and tension[121], chondrocytes are typically embedded in a highly hierarchical surrounding. Therefore, fiber alignment is supposed to have influence on cartilage regeneration. Subramanian et al. fabricated aligned chitosan fibers and found that, in addition to a higher elastic modulus, the oriented electrospun chitosan also provided better chondrocyte biocompatibility than the cast chitosan film [118]. Schneider and co-workers investigated the influence of the fiber orientation of electrospun scaffolds on the growth and ultrastructure of primary articular chondrocytes [115]. Their results showed that fiber alignment did not affect chondrocyte adhesion, cell alignment or production of cartilage-specific type II collagen. However, chondrocyte shape was affected by fiber alignment. On random fiber alignment, chondrocytes showed flatten shape, while the chondrocytes on scaffolds with aligned fibers exhibited a spindle-shaped morphology with rougher cell surfaces. Authors further suggest that the fiber diameter is another key parameter to mimic cartilage ECM structure and the diameter of electrospun nanofibers should be reduced from micrometer to about 300 nm in order to mimic the collagen fibers in cartilage ECM.

In addition, cartilage tissue has a special zonal organization of cells and ECM, which is important for its biomechanical function in diarthroidal joints [116, 119]. To mimic the zone-specific organization and mechanical properties of collagen fibrillar network in cartilage, McCullen and co-workers fabricated trilaminar scaffolds by sequential electrospinning and varying fiber size and orientation in a continuous construct [116]. This is an example that considers the fiber size, fiber orientation and shape of scaffolds simultaneously, and the trilaminar composite scaffolds showed similar key organizational characteristics of native cartilage, supported *in vitro* cartilage formation, and possessed superior mechanical properties to homogenous scaffolds, which indicates that the scaffolds with trilaminar structure possess great potential for repairing articular cartilage lesions. Although McCullen et al. has tried to mimic this structure by fabricating trilaminar scaffolds and investigated the cell responses to each specific structure *in vitro*, *in vivo* studies have not been

carried out yet.

3.1.6 Electrospun membranes with controlled structures for skin tissue engineering

Skin is composed of three layers: epidermis, dermis, and hypodermis, where different layer composes of different cells and provides different functions, which indicates that different structure of scaffolds may be needed for skin tissue engineering. Electrospinning has been used as an approach for developing scaffolds for engineered skin and wound dressings and the effects of nanofiber and membrane structures on cell behavior and ECM deposition have been studied [122, 123]. Kumbar et al. investigated the effect of fiber size on fibroblasts when they used electrospun PLGA as skin wound dressings [122]. They found that fibroblasts proliferated best and had spread morphology in the fiber range of 350 nm to 1100 nm and higher expression of type III collagen were found in scaffolds with fiber diameter in the above range. In addition to fiber diameter, Yang et al. investigated the effects of porosity and pore size on fibroblast migration and growth by fabricating PLGA and type I collagen composite electrospun scaffolds with high porosities and large pore sizes [123]. Results indicated that the high porosity in the scaffolds improved the migration of fibroblasts into scaffolds.

Even though there are several studies investigating the effects of electrospun scaffolds for skin tissue engineering, the effects of structure controlling of nanofibers on cell behavior for skin tissue engineering are relative less as compared to those for other tissue engineering. To our knowledge, only the above mentioned effects of nanofiber diameter and porous structure of membrane on fibroblasts have been studied. The effects of fiber alignment and fiber pattern on cell behavior and skin regeneration have not been reported yet. In addition, since skin has three layers and each layer involves different cells, more cell types should be considered as cell models in order to mimic the skin regeneration process. Finally, more *in vivo* studies should be carried out in order to test the properties of scaffolds in a similar environment to clinic applications.

3.2 Application of electrospun membranes with controlled structures in drug delivery

Electrospun membranes have also been widely studied for drug delivery applications. It has been accepted that the large surface area of electrospun membranes benefit drug encapsulation and delivery efficiency [13]. However, there is still space for controlling drug delivery behaviors in different applications of electrospun membranes. For example, controlling structures of the

electrospun nanofibers or membranes has been identified as an effective way to obtain drug delivery system with different drug release properties.

Most previous studies focused on the effects of electrospun nanofiber morphology, such as core/sheath structure and hollow structures on drug delivery. It has been reported that nanofibers with core/sheath structures present great potential applications in drug delivery, including growth factor delivery for tissue engineering [9-12, 43, 124]. The advantages of nanofibers with core/sheath structures in drug delivery have been demonstrated in many studies as following: (1) Drugs with different properties can be encapsulated and released simultaneously and independently, which means that biphasic drug release (BDR) can be realized. BDR is designed to release a drug at two different rates or in two different periods of time and often an immediate drug release followed by a sustained release, which is an ideal release behavior for the delivery of a wide variety pharmaceutical ingredients; (2) Some sensitive drugs that are easily to be denatured can be protected in core material; (3) Drug release behaviors can be controlled by core/sheath layers and the core-shell fibers could suppress the initial burst release and provide a sustained drug release useful for the release of growth factor or other therapeutic drugs. For example, Jiang et al. prepared a drug-loaded core–sheath PVP /zein nanofibers BRD using coaxial electrospinning [12]. In vitro ketoprofen (KET) release tests showed that the nanofibers could provide a typical BRD as there was an immediate release of 42.3% of the contained KET, followed by a sustained release over 10 h of the remaining drug. Su et al. prepared a compound P(LLA-CL) /collagen core/sheath nanofibers blended with bone morphogenetic protein 2 (BMP2) and dexamethasone (DEX) for controlled release during bone tissue engineering. P(LLA-CL) and BMP2 were in the core while collagen and DEX were in the sheath [9]. The authors indicated that the core/sheath structures could control the release behavior of different growth factors, e.g. DEX loaded into the shell layer showed a sharp initial burst release while BMP2 loaded into the core of the fiber resulted in slow and steady long-term release from coaxial electrospun fibers. This kind of release behavior can provide sustainable and sufficient amounts of growth factors throughout the entire release period, which benefits the viability, proliferation and osteogenic differentiation of human mesenchymal stromal cells.

Electrospun membranes with hollow nanofibers have been applied for drug delivery in order to enhance loading capacity and solve the problems of initial burst release and short-term release

of the electrospun fibrous membranes with solid nanofibers [39, 40]. For example, Wu et al. firstly applied membranes with NHAHF to deliver bovine serum albumin[40]. The results showed that the NHAHF has a highest loading capacity (96.8 mg/g) as compared to hydroxyapatite nanocrystal coated BGF and HAp nanocrystal coated porous BGF membranes. This loading capacity is also considerably high as compared with bovine serum albumin (BSA) loading efficiency of other form of HA. Besides, NHAHF has long-term sustained release property although there is an initial burst release due to the weak affinity of BSA in the hollow interior. In addition, hollow electrospun nanofibers with two different layers of wall also have advantages in drug delivery. Wei et al. have demonstrated that PES hollow ultrafine fibers with two layer wall possessed much larger delivery amounts and more stable release rate than that of PES porous ultrafine fibers. They concluded that hollow ultrafine fibers with two different layers of the fiber wall were more suitable as drug delivery materials as compared with porous ultrafine fibers [41].

Recently, the effects of nanofiber alignment and pattern on drug delivery have also been studied [125, 126]. Meng et al. found that the release rate of fenbufen from aligned PLGA/chitosan nanofibrous scaffold was lower than that from randomly oriented PLGA/chitosan nanofibrous scaffold, which indicated that the nanofiber arrangement would influence the release behavior [125]. Authors proposed that the aligned nanofibers enhanced the density of nanofibers and decreased the pore size of scaffolds compared with the randomly oriented nanofibers. Then, the outwards diffusion rate of the drug from the scaffold with aligned nanofibers was lower than that from the scaffold with random nanofibers. In our previous study, we have reported that deposition of electrospun nanofiber in certain patterns on substrate carrying drugs can modify the hydrophobicity of the substrate surface and subsequently control drug release from the substrate as it is well known that drug delivery behavior could be controlled by adjusting surface wettability of the drug carrier surface. [126]. In that study, PVB electrospun membranes with various nanofibrous structures and patterns were deposited on PVB polymer films for controlling drug release from the PVB film by adjusting the micro/nanopatterned electrospun structures on the surface. We further demonstrated that the density, distribution and patterns of the deposited electrospun nanofibers on the surface of PVB films could alter the hydrophobicity of the PVB films and adjust the water contact angle from 80 to 153.2 $^{\circ}$C [126], which can be seen from Fig.8.
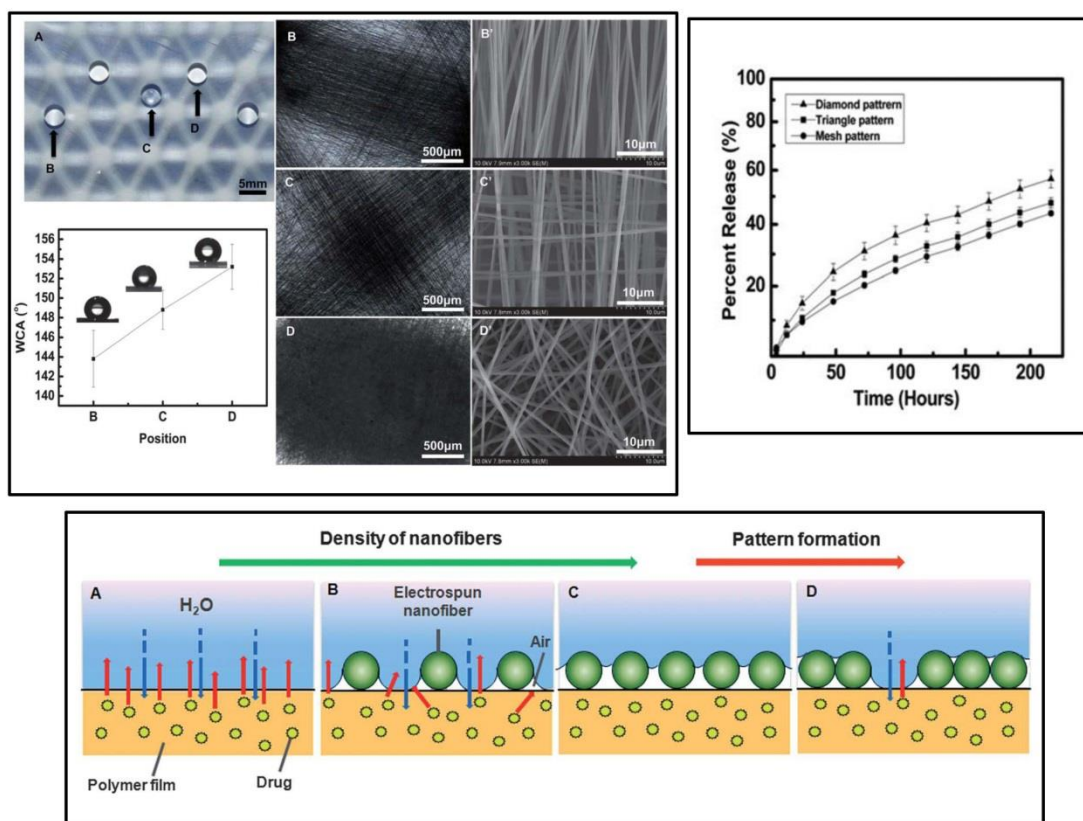
Fig. 8 Upper left panel: WCAs have different values at different places on the surface of the same micro-pattern. (A) Optical image of a water droplet set on different surface positions of the PVB film covered with the triangle pattern. The positions where droplets set on the edge of a triangle, the center of a triangle, and the node of the triangle network, are numbered as B, C and D, respectively. (B)–(D) are the enlarged optical views of the surface shown in (A). (B0), (C0) and (D0) are the SEM images of (B), (C) and (D), respectively. And the corresponding WCAs are 143.8 ± 2.9^{o}, 146.8 ± 2.0^{o}, 153.2 ± 2.3^{o} for positions B, C and D, which are shown in (E). Upper right panel: Acetaminophen release profiles of PVB films covered with mesh patterned (round dots), triangle patterned (squares) and diamond patterned (triangles) electrospun nanofibrous mats, respectively. Down panel: The effects of surface modification with electrospun nanofibrous structures and micro-patterns on the drug release from PVB polymer film at the early stage. (A) A pure PVB film without any surface modification; (B) a few electrospun nanofibers deposited onto the surface of the PVB film; (C) the density of deposited nanofibers increased; (D) the surface of the PVB film is modified by nanofibers with a micro-patterned structure. All these images were reproduced from [126].

4. Conclusions and future directions

Electrospun membranes are composed of nanofibers. Due to its advantages of easy fabrication, large surface area, nanofibrous structure mimics the natural ECM and topographic

guidance effect, electrospun membranes have been widely used in tissue engineering and drug delivery applications. With increased understanding of cell/material and drug/material interactions, more intention is now focused on preparing electrospun membranes with controlled multilevel hierarchical structure for tissue engineering and drug delivery applications. Efforts have been made to control structure of electrospun membranes from 1 dimensional structure of morphology, 2 dimensional structure of packing and alignment of nanofibers to 3 dimensional structure of pattern of nanofibers and shape of scaffolds using a number of physical and/or chemical methods as well as designation of setups.

In terms of controlling structures of electrospun membranes for tissue engineering, several challenges still remain. Previous studies usually focused on controlling of one or two structure of electrospun membranes. However, the fact is that various specific structures co-exist in one type of natural ECM. Therefore, one challenge is to fabricate porous scaffolds with structures similar to natural ECM in different levels at one time. The scaffold should have proper diameter of nanofibers, certain aligned and/or pattered nanofibers, together with a clinically relevant 3D shape, to thoroughly mimic the natural ECM of tissue to be regenerated. In addition, large pore size and high porosity of electropsun membranes for cell infiltration and migration and proper diameter of nanofibers that is identical to that of native ECM fibers (a diameter less than 100 nm, preferably in the range of 10-50 nm) also need to be considered. Furthermore, some special structure, such as core/sheath structure of nanofibers, may be chosen for encapsulating drugs or protein for anti-inflammation or improving tissue engineering.

The effects of morphology, diameter and secondary structure of single nanofibers, the alignment of nanofibers, stack of nanofibers and the pattern of nanofibers on the properties of the electrospun membranes as well as on cell behavior and tissue regeneration have been investigated. However, most of studies focused on the effects of the nanofiber and membrane structure on cell behavior, such as attachment, proliferation, differentiation, migration and orientation. The challenge is that it is critical to further understand the mechanisms through which the structure of nanofibers and membranes affects the cell behavior and further influences the tissue regeneration, among which the physiological and mechanotransductory signals need to be further investigated. These studies will help the material scientists to optimize the electrospun membranes for tissue regeneration.

In addition, although impressive progress has been made in obtaining electrospun scaffolds with high porosity to solve the problem of low cell infiltration rates, the mechanical properties and integrity of the scaffold are often compromised. Therefore, the cell infiltration rate may still remain very low. More recently, direct electrospinning or deposition of live cells has emerged as a novel technique to address this challenge [127-129]. For example, Seil and co-workers sprayed fibroblasts during the intervals of PLGA nanofiber electrospinning, which constructed a "cells-nanofibers" sandwich structure [127]. Jayasinghe and co-workers applied a coaxial electrospinning method for electrospinning of cells and fibers simultaneously [128, 129]. Highly concentrated cellular suspension was loaded in the inner capillary while the outer needle accommodated the flow of a PDMS medium, which took the advantages of core/shell structure of nanofiber. The cells located in the core of nanofibers can be protected by the outlayer of polymer. Both results indicate that the viability of the sprayed or electrospun cells was not affected by the fabrication process as a large population of the cells remained viable after electrospinning for a relatively long period of time, which indicate the feasibility to incorporate cells with electrospun scaffolds during the fabrication process and the low cell infiltration rate may be solved. However, electrospinning parameters need to be carefully chosen in order to maintain the cell viability.

Furthermore, the relationships between the drug controlled release profile and the structure of nanofibers and membranes need to be further elucidated. After being thoroughly studied, the release behavior of different drugs from different membranes with special structures should be precisely predicted or programmed so that different electrospun membranes can be used for delivering different drugs. Mathematical models of drug release from different nanofibers should be established and used to elucidate the underlying drug transport mechanism and predict the resulting drug release kinetics as a function of the nanofibers' structure.

Acknowledgement

References

1.   D. Li and Y. Xia, *Adv. Mater.*, 2006, 16, 1151-1170.

2.   R. Khajavi and M. Abbasipour, *Sci. Iran.*, 2012, 19, 2029-2034.

3.   W. Cui, Y. Zhou and J. Chang, *Sci. Technol. Adv. Mat.*, 2010, 11, 014108.

4.   M. Zamani, M. P. Prabhakaran and S. Ramakrishna, *Int. J. Nanomed.*, 2013, 8, 2997-3017.

5.   W. J. Lu, J. S. Sun and X. Y. Jiang, *J. Mater. Chem. B*, 2014, 2, 2369-2380.

6.   M. R. Ladd, T. K. Hill, J. J. Yoo and S. J. Lee, *Nanofibers - Production, Properties and Functional Applications*, 2011, DOI: 10.5772/24095., 347-372.

7.   X. Wang, B. Ding and B. Li, *Mater. Today*, 2013, 16, 229-241.

8.   Q. P. Pham, U. Sharma and A. G. Mikos, *Tissue Eng.*, 2006, 12, 1197-1211.

9.   Y. Su, Q. Su, W. Liu, M. Lim, J. R. Venugopal, X. Mo, S. Ramakrishna, S. S. Al-Deyab and M. El-Newehy, *Acta Biomater.*, 2012, 8, 763-771.

10.   Y. Yang, X. Li, L. Cheng, S. He, J. Zou, F. Chen and Z. Zhang, *Acta Biomater.*, 2011, 7, 2533-2543.

11.   D. G. Yu, X. Wang, X. Y. Li, W. Chian, Y. Li and Y. Z. Liao, *Acta Biomater.*, 2013, 9, 5665-5672.

12.   Y. N. Jiang, H. Y. Mo and D. G. Yu, *Int. J. Pharm.*, 2012, 438, 232-239.

13.   D.-G. Yu, *Health*, 2009, 01, 67-75.

14.   N. M. Neves, R. Campos, A. Pedro, J. Cunha, F. Macedo and R. Reis, *Int. J. Nanomed.*, 2007, 2, 433-448.

15.   A. Martins, M. L. Alves da Silva, S. Faria, A. P. Marques, R. L. Reis and N. M. Neves, *Macromol. Biosci.*, 2011, 11, 978-987.

16.   A. Guimarães, A. Martins, E. D. Pinho, S. Faria, R. Reis and N. M. Neves, *Nanomedicine*, 2010, 5, 539-554.

17.   Y. Ishii, H. Sakai and H. Murata, *Mater. Lett.*, 2008, 62, 3370-3372.

18.   Y. Z. Cai, G. R. Zhang, L. L. Wang, Y. Z. Jiang, H. W. Ouyang and X. H. Zou, *J.Biomed. Mater. Res. A*, 2012, 100, 1187-1194.

19.   B. Ding, M. R. Wang, X. F. Wang, J. Y. Yu and G. Sun, *Mater. Today*, 2010, 13, 16-27.

20.   X. F. Wang, B. Ding, J. Y. Yu and M. R. Wang, *Nano Today*, 2011, 6, 510-530.

21.   D. Gupta, J. Venugopal, M. P. Prabhakaran, V. R. Dev, S. Low, A. T. Choon and S. Ramakrishna, *Acta Biomater.*, 2009, 5, 2560-2569.

22.   D. C. Surrao, J. C. Fan, S. D. Waldman and B. G. Amsden, *Acta Biomater.*, 2012, 8, 3704-3713.

23.   C. M. Vaz, S. van Tuijl, C. V. Bouten and F. P. Baaijens, *Acta Biomater.*, 2005, 1, 575-582.

24.   A. Doustgani, E. Vasheghani-Farahani and M. Soleimani, *Nanomed. J.*, 2013, 1, 20-27.

25.   C. Y. Xu, R. Inai, M. Kotaki and S. Ramakrishna, *Biomaterials*, 2004, 25, 877-886.

26.   B. M. Baker, A. M. Handorf, L. C. Ionescu, W. J. Li and R. L. Mauck, *Expert Rev. Med. Devic.*, 2009, 6, 515-532.

27.   K. Nasouri, H. Bahrambeygi, A. Rabbi, A. M. Shoushtari and A. Kaflou, *J Appl Polym Sci*, 2012, 126, 127-135.

28.   Z. Sun, E. Zussman, A. L. Yuan, J. H. Wendorff and A. Greiner, *Adv. Mater.*, 2003, 15, 1929-1932.

29.   M. Wei, B. Kang, C. Sung and J. Mead, *Macromol. Mater. Eng.*, 2006, 291, 1307-1314.

30.   J. T. McCann, D. Li and Y. Xia, *J. Mater. Chem.*, 2005, 15, 735-738.

31.   J. M. Yang, L. S. Zha, D. G. Yu and J. Liu, *Colloid Surf. B: Biointerfaces*, 2013, 102, 737-743.

32.   A. V. Bazilevsky, A. L. Yarin and C. M. Megaridis, *Langmuir : the ACS journal of surfaces and colloids*, 2007, 23, 2311-2314.

33. T. T. T. Nguyen, O. H. Chung and J. S. Park, *Carbohydr. Polym.*, 2011, 86, 1799-1806.

34. D. Li and Y. Xia, *Nano Lett.*, 2004, 4, 933-938.

35. F. Bai, J. Wu, G. Gong, N. Sun, Y. Zhao and L. Jiang, *Chem. J. Chinese Univer.*, 2013, 34, 751-759.

36. P. Liu, J. Ma, J. Gong and J. Xu, *Adv. Mater. Res.*, 2013, 750-752, 236-240.

37. X. Xia, X. J. Dong, Q. F. Wei, Y. B. Cai and K. Y. Lu, *eXPRESS Polym. Lett.*, 2011, 6, 169-176.

38. J. Zhang, S. W. Choi and S. S. Kim, *J. Solid State Chem.*, 2011, 184, 3008-3013.

39. H. Yang and L. Dong, *Micro Electro Mechanical Systems (MEMS), 2010 IEEE 23rd International Conference*, 2010, DOI: 10.1109/MEMSYS.2010.5442505, 308-311.

40. L. Wu, Y. Dou, K. Lin, W. Zhai, W. Cui and J. Chang, *Chem Commun (Camb)*, 2011, 47, 11674-11676.

41. Z. Wei, Q. Zhang, M. Peng, X. Wang, S. long and J. Yang, *Colloid Polym. Sci.*, 2014, DOI: 10.1007/s00396-014-3187-y, 1-7.

42. J. B. Lee, S. I. Jeong, M. S. Bae, D. H. Yang, D. N. Heo, C. H. Kim, E. Alsberg and I. K. Kwon, *Tissue Eng. A*, 2011, 17, 2695-2702.

43. T. T. Nguyen, C. Ghosh, S. G. Hwang, N. Chanunpanich and J. S. Park, *Int. J. Pharm.* , 2012, 439, 296-306.

44. Y. Z. Zhang, Y. Feng, Z.-M. Huang, S. Ramakrishna and C. T. Lim, *Nanotechnology*, 2006, 17, 901.

45. M. Bogntizki, T. Frese, M. Steinhart, A. Greiner and J. H. Wendorff, *Polym Eng Sci*, 2001, 41, 982-989.

46. C. Hellmann, J. Belardi, R. Dersch, A. Greiner, J. H. Wendorff and S. Bahnmueller, *Polymer*, 2009, 50, 1197-1205.

47. S. Megelski, J. S. Stephens, D. B. Chase and J. F. Rabolt, *Macromolecules*, 2002, 35, 8456-8466.

48. G. T. Christopherson, H. Song and H. Q. Mao, *Biomaterials*, 2009, 30, 556-564.

49. H. B. Wang, M. E. Mullins, J. M. Cregg, C. W. McCarthy and R. J. Gilbert, *Acta Biomater.*, 2010, 6, 2970-2978.

50. J. M. Du, S. Shintay and X. W. Zhang, *J. Polym. Sci., Part B: Polym. Phys.*, 2008, 46, 1611-1618.

51. C. J. Thompson, G. G. Chase, A. L. Yarin and D. H. Reneker, *Polymer*, 2007, 48, 6913-6922.

52. C. Mit-uppatham, M. Nithitanakul and P. Supaphol, *Macromol Symp*, 2004, 216, 293-299.

53. G. C. Rutledge and S. V. Fridrikh, *Adv. Drug. Deliv. Rev.*, 2007, 59, 1384-1391.

54. K. H. Lee, H. Y. Kim, H. J. Bang, Y. H. Jung and S. G. Lee, *Polymer*, 2003, 44, 4029-4034.

55. J. M. Deitzel, J. Kleinmeyer, D. Harris and N. C. B. Tan, *Polymer*, 2001, 42, 261-272.

56. R. Liu, N. Cai, W. Yang, W. Chen and H. Liu, *J Appl Polym Sci*, 2009, 116, NA-NA.

57. W. Huang, M.-J. Wang, C.-L. Liu, J. You, S.-C. Chen, Y.-Z. Wang and Y. Liu, *J. Mater. Chem. A*, 2014, 2, 8416.

58. T. G. Kim, H. J. Chung and T. G. Park, *Acta Biomater.*, 2008, 4, 1611-1619.

59. J. Wu, C. Huang, W. Liu, A. L. Yin, W. Chen, C. He, H. Wang, S. Liu, C. Fan, G. L. Bowlin and X. Mo, *J. Biomed. Nanotechnol.*, 2014, 10, 603-614.

60. C. Vaquette and J. J. Cooper-White, *Acta Biomater.*, 2011, 7, 2544-2557.

61. M. F. Leong, M. Z. Rasheed, T. C. Lim and K. S. Chian, *J. Biomed. Mater. Res. A*, 2009, 91, 231-240.

62. B. M. Baker, A. O. Gee, R. B. Metter, A. S. Nathan, R. A. Marklein, J. A. Burdick and R. L. Mauck,

Biomaterials, 2008, 29, 2348-2358.

63. M. C. Phipps, W. C. Clem, J. M. Grunda, G. A. Clines and S. L. Bellis, *Biomaterials*, 2012, 33, 524-534.

64. B. A. Blakeney, A. Tambralli, J. M. Anderson, A. Andukuri, D. J. Lim, D. R. Dean and H. W. Jun, *Biomaterials*, 2011, 32, 1583-1590.

65. M. J. McClure, P. S. Wolfe, D. G. Simpson, S. A. Sell and G. L. Bowlin, *Biomaterials*, 2012, 33, 771-779.

66. J. Rnjak-Kovacina and A. S. Weiss, *Tissue Eng. B: Reviews*, 2011, 17, 365-372.

67. A. Thorvaldsson, H. Stenhamre, P. Gatenholm and P. Walkenstrom, *Biomacromolecules*, 2008, 9, 1044-1049.

68. L. S. Carnell, E. J. Siochi, N. M. Holloway, R. M. Stephens, C. Rhim, L. E. Niklason and R. L. Clark, *Macromolecules*, 2008, 41, 5345-5349.

69. M. V. Jose, V. Thomas, K. T. Johnson, D. R. Dean and E. Nyairo, *Acta Biomater.*, 2009, 5, 305-315.

70. H. Pan, L. Li, L. Hu and X. Cui, *Polymer*, 2006, 47, 4901-4904.

71. J. S. Kim and D. H. Reneker, *Polym Eng Sci*, 1999, 39, 849-854.

72. P. Katta, M. Alessandro, R. D. Ramsier and G. G. Chase, *Nano Lett.*, 2004, 4, 2215-2218.

73. D. Li, Y. Wang and Y. Xia, *Nano Lett.*, 2003, 3, 1167-1171.

74. G. Kim and W. Kim, *J. Manuf. Sci. Eng.*, 2008, 130, 021006,021001-021006.

75. A. Theron, E. Zussman and A. L. Yarin, *Nanotechnology*, 2001, 12, 384-390.

76. D. Li, Y. Wang and Y. Xia, *Adv. Mater.*, 2004, 16, 361-366.

77. D. Li, G. Ouyang, J. T. McCann and Y. Xia, *Nano Lett.*, 2005, 5, 913-916.

78. J. Xie, M. R. MacEwan, W. Z. Ray, W. Liu, D. Y. Siewe and Y. Xia, *ACS Nano*, 2010, 4, 5027-5036.

79. B. T. Song, W. G. Cui and J. Chang, *J Appl Polym Sci*, 2011, 122, 1047-1052.

80. D. Zhang and J. Chang, *Adv. Mater.*, 2007, 19, 3664-3667.

81. Y. Wang, G. Wang, L. Chen, H. Li, T. Yin, B. Wang, J. C. Lee and Q. Yu, *Biofabrication*, 2009, 1, 015001.

82. D. Zhang and J. Chang, *Nano Lett.*, 2008, 8, 3283-3287.

83. H. Xu, W. Cui and J. Chang, *J Appl Polym Sci*, 2013, 127, 1550-1554.

84. D. C. Surrao, J. W. S. Hayami, S. D. Waldman and B. G. Amsden, *Biomacromolecules*, 2010, 11, 3624-3629.

85. D. C. Surrao, S. D. Waldman and B. G. Amsden, *Acta Biomater.*, 2012, 8, 3997-4006.

86. Y. Wang, H. Shi, J. Qiao, Y. Tian, M. Wu, W. Zhang, Y. Lin, Z. Niu and Y. Huang, *ACS Appl. Mater. Inter.*, 2014, 6, 2958-2962.

87. C. Del Gaudio, L. Fioravanzo, M. Folin, F. Marchi, E. Ercolani and A. Bianco, *J. Biomed. Mater. Res. Part B: Appl. Biomater.*, 2012, 100, 1883-1898.

88. J. Stitzel, J. Liu, S. J. Lee, M. Komura, J. Berry, S. Soker, G. Lim, M. Van Dyke, R. Czerw, J. J. Yoo and A. Atala, *Biomaterials*, 2006, 27, 1088-1094.

89. H. Wu, J. Fan, C. C. Chu and J. Wu, *J. Mater. Sci. - Mater. Med.*, 2010, 21, 3207-3215.

90. M. Deng, S. G. Kumbar, L. S. Nair, A. L. Weikel, H. R. Allcock and C. T. Laurencin, *Adv. Funct. Mater.*, 2011, 21, 2601-2601.

91. C. M. Valmikinathan, J. Tian, J. Wang and X. Yu, *J. Neural. Eng.*, 2008, 5, 422-432.

92. L. He, S. Liao, D. Quan, K. Ma, C. Chan, S. Ramakrishna and J. Lu, *Acta Biomater.*, 2010, 6, 2960-2969.

93.   X. Zhang, X. Gao, L. Jiang and J. Qin, *Biomicrofluidics*, 2011, 5, 32007-3200710.

94.   F. Yang, R. Murugan, S. Wang and S. Ramakrishna, *Biomaterials*, 2005, 26, 2603-2610.

95.   J. Xie, M. R. MacEwan, A. G. Schwartz and Y. Xia, *Nanoscale*, 2010, 2, 35-44.

96.   S. H. Lim, X. Y. Liu, H. Song, K. J. Yarema and H. Q. Mao, *Biomaterials*, 2010, 31, 9031-9039.

97.   S. Y. Chew, R. Mi, A. Hoke and K. W. Leong, *Biomaterials*, 2008, 29, 653-661.

98.   J. M. Corey, D. Y. Lin, K. B. Mycek, Q. Chen, S. Samuel, E. L. Feldman and D. C. Martin, *J. Biomed. Mater. Res. A*, 2007, 83, 636-645.

99.   Y. Liu, L. Zhang, H. Li, S. Yan, J. Yu, J. Weng and X. Li, *Langmuir : the ACS journal of surfaces and colloids*, 2012, 28, 17134-17142.

100.   J. Xie, M. R. MacEwan, X. Li, S. E. Sakiyama-Elbert and Y. Xia, *ACS Nano*, 2009, 3, 1151-1159.

101.   T. B. Bini, S. Gao, S. Wang and S. Ramakrishna, *J. Mater. Sci. Mater. Med.*, 2005, 16, 367-375.

102.   Y. Zhu, A. Wang, S. Patel, K. Kurpinski, E. Diao, X. Bao, G. Kwong, W. Young and S. Li, *Tissue Eng. Part C Methods.*, 2011, 17, 705-715.

103.   W. Liu, S. Thomopoulos and Y. Xia, *Advanced healthcare materials*, 2012, 1, 10-25.

104.   G. Ma, D. Fang, Y. Liu, X. Zhu and J. Nie, *Carbohydr. Polym.*, 2012, 87, 737-743.

105.   R. Chen, C. Huang, Q. Ke, C. He, H. Wang and X. Mo, *Colloid Surf. B: Biointerfaces*, 2010, 79, 315-325.

106.   Y. Li, F. Chen, J. Nie and D. Yang, *Carbohydr. Polym.*, 2012, 90, 1445-1451.

107.   A. S. Badami, M. R. Kreke, M. S. Thompson, J. S. Riffle and A. S. Goldstein, *Biomaterials*, 2006, 27, 596-606.

108.   W. J. Li, R. L. Mauck, J. A. Cooper, X. N. Yuan and R. S. Tuan, *J Biomech*, 2007, 40, 1686-1693.

109.   J. Wang, C. M. Valmikinathan, W. Liu, C. T. Laurencin and X. Yu, *J. Biomed. Mater. Res. A*, 2010, 93, 753-762.

110.   C. H. Lee, H. J. Shin, I. H. Cho, Y. M. Kang, I. A. Kim, K. D. Park and J. W. Shin, *Biomaterials*, 2005, 26, 1261-1270.

111.   X. Li, J. Xie, J. Lipner, X. Yuan, S. Thomopoulos and Y. Xia, *Nano Lett.*, 2009, 9, 2763-2768.

112.   J. Xue, B. Feng, R. Zheng, Y. Lu, G. Zhou, W. Liu, Y. Cao, Y. Zhang and W. J. Zhang, *Biomaterials*, 2013, 34, 2624-2631.

113.   H. Liu, X. Ding, G. Zhou, P. Li, X. Wei and Y. Fan, *J Nanomaterials*, 2013, Article ID 495708, 11 pages.

114.   Q. P. Pham, U. Sharma and A. G. Mikos, *Electrospinning of polymeric nanofibers for tissue engineering applications: a review*, 2006.

115.   T. Schneider, B. Kohl, T. Sauter, K. Kratz, A. Lendlein, W. Ertel and G. Schulze-Tanzil, *Clin Hemorheol Microcirc*, 2012, 52, 325-336.

116.   S. D. McCullen, H. Autefage, A. Callanan, E. Gentleman and M. M. Stevens, *Tissue Eng. Part A.*, 2012, 18, 2073-2083.

117.   S. Liao, B. Li, Z. Ma, H. Wei, C. Chan and S. Ramakrishna, *Biomed. Mater.*, 2006, 1, R45-53.

118.   A. Subramanian, D. Vu, G. F. Larsen and H.-Y. Lin, *J Biomater. Sci. Polym. Ed.*, 2005, 16.

119.   T. B. Woodfield, C. A. Van Blitterswijk, J. De Wijn, T. J. Sims, A. P. Hollander and J. Riesle, *Tissue Eng.*, 2005 11, 1297-1311.

120.   R. Zheng, H. Duan, J. Xue, Y. Liu, B. Feng, S. Zhao, Y. Zhu, A. He, W. Zhang, W. Liu, Y. Cao and G. Zhou, *Biomaterials*, 2014, 35, 152-164.

121.   J. J. Cassidy, A. Hiltner and E. Baer, *Hierarchical structure of the intervertebral disc*, 1989.

122.   S. G. Kumbar, S. P. Nukavarapu, R. James, L. S. Nair and C. T. Laurencin, *Biomaterials*, 2008, 29,

4100-4107.

123.   Y. Yang, X. L. Zhu, W. G. Cui, X. H. Li and Y. Jin, *Macromol. Mater. Eng.*, 2009, 294, 611-619.

124.   C. L. He, Z. M. Huang and X. J. Han, *J. Biomed. Mater. Res. A*, 2009, 89, 80-95.

125.   Z. X. Meng, W. Zheng, L. Li and Y. F. Zheng, *Mater. Chem. Phys.*, 2011, 125, 606-611.

126.   H. Xu, H. Li and J. Chang, *J Mater. Chem. B*, 2013, 1, 4182.

127.   J. T. Seil and T. J. Webster, *Int. J. Nanomed.*, 2011, 6, 1095-1099.

128.   S. N. Jayasinghe, S. Irvine and J. R. McEwan, *Nanomedicine (Lond)*, 2007., 2, 555-567.

129.   A. Townsend-Nicholson and S. N. Jayasinghe, *Biomacromolecules*, 2006, 7, 3364-3369.